AT₂R stimulation with C21 prevents arterial stiffening and endothelial dysfunction in the abdominal aorta from mice fed a high-fat diet

Raquel González-Blázquez[1], Martín Alcalá[2], José Miguel Cárdenas-Rebollo[3], Marta Viana[2], Ulrike Muscha Steckelings[4], William A. Boisvert[5,6], Thomas Unger[7], María S. Fernández-Alfonso[8,9], Beatriz Somoza[1]* and Marta Gil-Ortega[1]*

[1]Departamento de Ciencias Farmacéuticas y de la Salud, Facultad de Farmacia, Universidad San Pablo-CEU, CEU Universities, 28925, Madrid, Spain. [2]Departamento de Química y Bioquímica, Facultad de Farmacia, Universidad CEU-San Pablo, CEU Universities, 28925, Madrid, Spain. [3]Departamento de Matemática Aplicada y Estadística. Facultad de Ciencias Económicas y Empresariales. Universidad San Pablo-CEU, CEU Universities, 28925, Madrid, Spain. [4]Department of Cardiovascular and Renal Research, Institute of Molecular Medicine, University of Southern Denmark, Odense, Denmark. [5]Center for Cardiovascular Research, John A. Burns School of Medicine, University of Hawaii, 651 Ilalo Street, BSB311, Honolulu, HI 96813, USA. [6]Institute of Fundamental Medicine and Biology, Kazan Federal University, 18 Kremlevskaya Str., Kazan 420008, Russia. [7]CARIM - School for Cardiovascular Diseases, Maastricht University, Maastricht, The Netherlands. [8]Instituto Pluridisciplinar, Unidad de Cartografía Cerebral, Universidad Complutense de Madrid, 28040 Madrid, Spain. [9]Departamento de Farmacología, Facultad de Farmacia, Universidad Complutense de Madrid, 28040 Madrid, Spain.

* These authors contributed equally to this work.

Short title: C21 prevents obesity-induced vascular alterations

Corresponding author:

Beatriz Somoza Hernández

Universidad CEU San Pablo, Facultad de Farmacia

Ctra. Boadilla del Monte Km 5.300, 28925, Alcorcón, Madrid (Spain)

Telephone number: (+34) 913724700

Fax number: (+34) 913724775

e-mail address: bsomoza.fcex@ceu.es

ABSTRACT

The aim of this study was to evaluate the effect of Compound 21 (C21), a selective AT_2R agonist, on the prevention of endothelial dysfunction, extracellular matrix (ECM) remodeling and arterial stiffness associated with diet-induced obesity (DIO).

5-week-old male C57BL/6J mice were fed a standard (Chow) or high-fat diet (HF) for 6 weeks. Half of the animals of each group were simultaneously treated with C21 (1mg/kg/day, in the drinking water), generating 4 groups: Chow C, Chow C21, HF C, HF C21. Vascular function and mechanical properties were determined in the abdominal aorta. To evaluate ECM remodeling, collagen deposition, activity of metalloproteinases (MMP) 2 and 9 and TGF-β_1 concentration were analyzed in the plasma. Abdominal aortas from HF C mice showed endothelial dysfunction as well as enhanced contractile but reduced relaxant responses to Ang II. This effect was abrogated with C21 treatment by preserving NO availability. A left-shift in the tension-stretch relationship, paralleled by an augmented β-index (marker of intrinsic arterial stiffness), and enhanced collagen deposition and MMP-2/-9 activities were also detected in HF mice. However, when treated with C21, HF mice exhibited lower TGF-β1 levels in abdominal aortas together with reduced MMP activities and collagen deposition compared with HF C mice.

In conclusion, these data demonstrate that AT_2R stimulation by C21 in obesity preserves NO availability and prevents unhealthy vascular remodeling, thus protecting the abdominal aorta in HF mice against the development of endothelial dysfunction, ECM remodeling and arterial stiffness.

KEYWORDS: Compound 21, endothelial dysfunction, angiotensin type 2 receptor, arterial stiffness, obesity, collagen

NON-STANDARD ABBREVIATIONS AND ACRONYMS ACh: acetylcholine; Ang: angiotensin; AT_1R: angiotensin II type 1 receptor; AT_2R: angiotensin II type 2 receptor; B_2R; bradykinin type 2 receptor; BW: body weight; C21: Compound 21; CVD: cardiovascular disease; DIO: diet-induced obesity; ECM: extracellular matrix; EI: energy intake; HF: high-fat; MasR: Mas receptor; MMP: metalloproteinases; Phe: phenylephrine; PWV: pulse wave velocity; RAS: renin angiotensin system; WI: water intake.

1. INTRODUCTION

Obesity constitutes a known risk factor for the development of vascular damage[1] including endothelial dysfunction, vascular remodeling and arterial stiffness[2-5]. Endothelial dysfunction has been traditionally considered as one of the earliest vascular alterations developed during the onset of obesity. Numerous studies performed in obese humans[6, 7] and rodents[2, 3, 8] have revealed that endothelial dysfunction is mainly due to a reduction of NO availability[3, 5, 9]. We have recently shown that the renin angiotensin system plays a key role in the upstream signaling cascade of NO production. Our data demonstrate that in obesity, the crosstalk between the angiotensin II type 2 receptor (AT_2R), type 2 bradykinin receptor (B_2R) and Mas receptor (MasR) is interrupted, which in turn inhibits the Akt/eNOS and the PKA/eNOS pathways[5].

Increasing evidence suggests that vascular remodeling and arterial stiffness, the other two major factors in vascular damage, can be also considered as early markers of cardiovascular disease (CVD)[10, 11]. Moreover, arterial stiffness has emerged as an independent risk predictor of cardiovascular morbimortality[12, 13]. Systemic arterial stiffness, determined with pulse wave velocity (PWV) is increased in obese patients[14-18] and mouse models of diet-induced obesity (DIO)[4, 19-21]. Similarly, intrinsic arterial stiffness assessed with the β-index[22] is currently used as a predictor of CVD[23] and precedes the development of systemic arterial stiffness[24]. Among the main mechanisms involved in obesity-induced arterial stiffening, extracellular matrix (ECM) remodeling must be highlighted[19]. In this regard, we have recently demonstrated an increased collagen deposition together with an impaired elastin organization in mesenteric arteries from obese mice[4]. Moreover, metalloproteinases (MMP, mainly the 2 and 9 isoforms) are known to play a key role in ECM degradation[25], thus contributing to elastolysis[26] and collagen deposition in the arterial wall[27]. It is important to note that the abdominal aorta presents an increased collagen/elastin ratio [28, 29], which makes it structurally more vulnerable to vascular alterations and to the development of cardiovascular disorders like aneurysms[30, 31].

As an important cytokine involved in vascular function, TGF-β_1 constitutes the main growth factor involved in fibrotic processes and collagen deposition[32] whose activation may be mediated by the actions of MMP-2 and MMP-9[33]. In addition, angiotensin II (Ang II) has been shown to regulate TGF-β expression and synthesis, and to increase the levels of active TGF-β_1 in obesity[34]. TGF–β_1 might also potentiate AT_1R-mediated effects elicited by Ang II, thus accounting for ECM remodeling and fibrosis, likely caused by an overactivation of MMPs[35, 36]. Consequently, obesity-induced AT_1R overactivation could be responsible for obesity-induced arterial stiffening[37, 38].

Compound 21 (C21), a selective non-peptidic agonist of the AT_2R elicits vasodilatory, anti-fibrotic, anti-inflammatory and antioxidant responses in several organs[39]. Intriguingly, an accelerated collagen deposition has been described in AT_2R knockout mice and when the AT_2R is blocked by a specific AT_2R antagonist, PD123319[40, 41]. In addition, several studies have suggested that C21 may cause increased expression and activity of the tissue inhibitor metalloproteinases 1 and 2 (TIMP-1 and TIMP-2) which could in turn inhibit MMP-9 and MMP-2 and collagen accumulation[42, 43].

In the present study, we hypothesize that obesity induces the development of arterial stiffness due to a reduction of endothelial NO levels and ECM remodeling, and that this could be prevented by the treatment with C21. We therefore tested whether C21 might preserve endothelial function and arterial distensibility in the abdominal aorta from DIO mice. In addition, we assessed the mechanisms involved on the potential beneficial vascular effects derived from AT_2R activation.

2. METHODS

2.1. Animal model design

Experiments were conducted in 4-week-old male C57BL/6J mice inbred in the animal facilities from Universidad San Pablo-CEU, and previously used in the study performed by González-Blázquez et al.[5]. Animals were placed in individual cages and housed under controlled light (12:12 h light-dark cycles), temperature (22-24 °C) and relative humidity (44-55%) conditions. Animals had free access to standard food and water *ad libitum* for one week of acclimation. Thereafter, animals were assigned to a control chow diet (Chow;Teklad Rodent Diet 2918, 18 % of Kcal from fat; 3.1 Kcal/g; Envigo, USA) or to a high-fat diet (HF; D12451, 62 % of kcal from fat; 5.1 kcal/g; Test Diet, UK) for 6 weeks. Half of the animals of each group were simultaneously treated with Compound 21 (C21; 1 mg/kg/day in the drinking water), generating 4 experimental groups; Chow C, Chow C21, HF C, HF C21.

Body weight (BW) and food intake were monitored twice a week. To calculate the dose of C21 accurately, water intake was monitored daily. Energy consumption was also assessed and expressed as Kcal/day/mice. After 6 weeks of diet and treatment, mice were weighed and euthanized at 9 am by decapitation under inhalational anesthesia with isoflurane (5%). Blood samples were collected in chilled heparin-coated polypropylene tubes and centrifuged at 800G for 10 min at 4ºC to obtain plasma, that was stored at -80ºC. The abdominal aorta was immediately dissected and placed in ice-cold Krebs-Henseleit solution (KHS;115 mmol/L NaCl, 4.6 mmol/L KCl, 2.5 mmol/L $CaCl_2$, 25 mmol/L $NaHCO_3$, 1.2 mmol/L KH_2PO_4, 1.2 mmol/L $MgSO_4$, 0.01 mmol/L EDTA and 5.5 mmol/L glucose) for vascular function and mechanical studies. Other aortic segments were snap-frozen in liquid nitrogen and kept at -80ºC.

All experiments were performed in accordance with the European Union Laboratory Animal Care Rules (86/609/ECC directive) and approved by the Ethical Committe of the San Pablo CEU University and the Animal Protection Area of the Comunidad Autónoma de Madrid (PROEX 200/18).

2.2. Assessment of vascular function and mechanics

Abdominal aorta was gently cleaned of fat and connective tissue and cut into 2-mm-length segments. Vascular function was studied by isometric tension recording in abdominal aorta segments, as previously described[44]. Arterial contractility was assessed with potassium chloride (KCl, 60 mmol/L). Concentration-response curves to Ang II, 10^{-9}-10^{-6} mol/L) were carried out to analyze contractile responses to Ang II. Relaxation curves to Ang II (10^{-9}-10^{-6} mol/L) were also performed in segments pre-incubated with Losartan (AT_1R antagonist, 10^{-7} mol/L, 20 min) and pre-contracted with phenylephrine (Phe, 10^{-6} mol/L). In addition, endothelial function was analyzed by performing concentration-response curves to acetylcholine (ACh, 10^{-9}-10^{-4} mol/L) in aortic rings previously contracted with Phe (10^{-6} mol/L). Some rings were pre-incubated with NG-nitro-L-arginine methyl ester (L-NAME, NOS inhibitor, 10^{-4} mol/L), PD123177 (AT_2R antagonist, 10^{-7} mol/L), A779 (MasR, antagonist, 10^{-6} mol/L) or HOE-140 (B_2R antagonist, 10^{-6} mol/L) for 5 min (A779) or 20 min (L-NAME, PD123177 and HOE-140) before adding Ang II or ACh.

Thereafter, abdominal segments were washed 3 times with Ca^{2+}-free KHS (115 mmol/L NaCl, 4.6 mmol/L KCl, 25 mmol/L $NaHCO_3$, 1.2 mmol/L KH_2PO_4, 1.2 mmol/L $MgSO_4$, 0.01 mmol/L EDTA, 10 mmol/L EGTA and 5.5 mmol/L glucose) to remove Ca^{2+} and mechanical properties were then tested in aortic rings using an isometric recording system as described by Angus & Right in 2000[45] in Ca^{2+}-free KHS. After 15 min of equilibration period with segments unstretched (with both wires in contact with the inner wall of the rings but not generating any detectable force), the distance between the wires was increased in 200 μm steps with a micrometer every 3 min and the force was registered just before each stretch. This procedure was stopped when the system reached the maximal stretch allowed or when the tissue failed. β-index, was calculated as the slope of the tension-stretch relationship, derived from the expression $T_i = a \cdot e^{\beta \cdot L_i}$, as previously described[46].

2.3. Gene expression analysis

Fragments of the abdominal aorta were used for RNA extraction from 3-4 independent samples of each group. Samples were processed using Trizol Reagent (Invitrogen, USA) and a Illustra Rnaspin mini-isolation kit (Cytiva, USA). The concentration and purity of the extracted RNA were determined spectrophotometrically. The integrity of the RNA was assessed by gel electrophoresis. Reverse transcription was performed on 100 ng of RNA with PrimeScript™ RT Reagent Kit (Takara Bio, Japan) using random hexamer primers and oligod(T) primers. qPCR analyses were performed in a CXF96 thermocycler (Bio-Rad laboratories, USA). 6.25 ng of cDNA were run in duplicate, and the mRNA levels were determined using 500 nM intron-skipping primers (sequences are listed in the Supplemental Table 1), SYBR Green Master Mix (Takara Bio, Japan). Tata-box binding protein (*Tbp*) and glyceraldehyde-3-phosphate dehydrogenase (*Gapdh*) were selected as housekeeping genes. The expression of Chow C group was set as 1 and relative expression was calculated using the Pfaffl method[47].

2.4. Determination of collagen deposition in the abdominal aorta by immunofluorescence and fluorimetric assay

Aortic segments were fixed in 4% paraformaldehyde [60 min; room temperature (RT)], washed with 0.2% Tween-20 in PBS (15 min; RT) and incubated with blocking solution (3% BSA in PBS; 30 min; RT). Thereafter, abdominal rings were incubated with collagen type I and type III antibodies (1:50; Abcam, Germany; overnight; 4ºC) in immunofluorescence buffer (1% BSA, 0.2% Triton and 0.05% Tween-20 in PBS). Then, segments were washed and incubated with the secondary antibody Alexa-Fluor 555 (1:200; Invitrogen, USA; 60 min; RT). Intact arterial segments were mounted as previously described[48] and visualized by confocal microscopy (Leica TCS SP5). Stacks of serial optical sections were captured from 3 randomly chosen regions with a x63 objective at zoom 2, under identical conditions of laser intensity,

brightness, and contrast[49]. Fluorescence intensity was quantified with ImageJ software (NIH, USA, Version 1.50f).

Total collagen content was also assessed in abdominal aorta homogenates with a specific fluorimetric assay (MAK322, Sigma-Aldrich, Spain).

2.5. Determination of TGF-β_1 in the abdominal aorta

TGF-β_1 concentrations were analysed in the same tissue homogenates used for the fluorimetric quantification of collagen by means of a specific ELISA kit for TGF-β_1 (SEA124Mu; Cloud-Clone Corp. S.L., USA; < 10% intraassay and < 12% interassay variation).

2.6. Analysis of MMP-2 and MMP-9 activities by gelatin zymography

Plasma samples (4 μg of proteins) were used for MMP-2 and MMP-9 activity assays. Briefly, samples were mixed with Laemmli solution [for a final concentration of 0.025 mol/L Tris (pH 6.8), 5% glycerol, 0.4% SDS, and 0.002% bromophenol blue] and loaded to SDS-polyacrylamide gels electrophoresis (PAGE) containing 0.0008% gelatin. After several washing steps with distilled water, gels were incubated with the enzymatic activation buffer (50 mmol/L Tris-HCl, 6 mmol/L CaCl$_2$ and 2.5% Triton X-100; 1h; RT) and then with Triton X-100-free enzymatic activation buffer (24h; 37°C). Gels were stained with Coomassie Brilliant Blue (BioRad, USA; 10 min; RT) and distained with 40% methanol/10% acetic acid in distilled water (1 min). Then, gels were incubated with a stop solution (10% acetic acid; 24–48 h, as required) and visualized with ChemiDoc XRS+ Imaging System (BioRad, USA). Gelatinolytic activity of MMP-2 and -9 was quantified as previously described[50] (Image Lab 6.0 software, BioRad USA).

2.7. Chemicals

ACh and L-NAME were dissolved in saline, Phe in 0.01% ascorbic acid/saline and Ang II, Losartan and C21 in distilled water. All reagents were provided by Sigma Aldrich (Spain), except C21, provided by Vicore Pharma (Sweden).

2.8. Data analysis

Contractile responses to Ang II were expressed as the percentage of the maximal contractile response induced by KCl. Relaxant responses were expressed as the percentage of previous contraction to Phe. The maximal response (E_{max}) and the potency (pD_2) were determined by a non-linear regression analysis of each individual concentration-response curve to ACh or Ang II. Area under the curves (AUC) were calculated from the individual concentration-response curve plots.

Data are expressed as mean ± SEM and n denote the number of replicates for each experiment. The outliers were identified through the Rout method, using a Q=1%. The normal distribution of each variable was verified with the Shapiro-Wilk and Kolmogorov-Smirnov tests. Statistical differences ($p<0.05$) between the experimental groups were assessed using a one-way analysis of the variance test (1-ANOVA) followed by a Dunnett´s multiple comparison test for Gaussian distributions. For those comparison involving two variables, two-way ANOVA (2-ANOVA) followed by Tukey´s multiple comparison test was used. Correlation analyses were performed through linear regression and analyzed by Pearson's correlation. All statistical analyses were performed using GraphPad Prism (version7) software (San Diego, USA).

3. **RESULTS**

3.1. Effect of HF-feeding and C21 treatment on BW and food intake

As expected, and as it has been previously described[5], BW increase was significantly higher in HF than in Chow animals. The treatment with C21 did not affect BW gain either in the Chow nor in the HF group. Similarly, energy intake (EI), expressed as Kcal/mouse/day, was significantly enhanced by HF feeding but unmodified by the treatment with C21. Interestingly, a significant reduction in water intake (WI) was also detected in HF mice, independently of the treatment with C21 (Table 1).

3.2. C21 prevents the development of endothelial dysfunction in HF mice through NO overproduction

In order to study the contractile capacity of the aortic segments, they were pre-constricted with KCl (60 mmol/L) and Phe (10^{-6} mol/L). No differences were observed in the contractile response to these agents in the different groups (Suppl Table 2).

HF C mice exhibited a significant reduction in endothelial-dependent relaxation to ACh compared with Chow C animals, as evidenced by E_{max} values (E_{max}HF C = 57.1±1.9 *vs* E_{max}Chow C = 76.4±3.3; p<0.001; Figure 1A). Interestingly, HF C21 mice showed higher relaxant responses than HF C mice (E_{max}HF C21= 67.6±2.2 *vs* E_{max}HF C = 57.1±1.9; p<0.05; Figure 1A) but similar to Chow C group, thus indicating a protective effect of C21 on the development of obesity-induced endothelial dysfunction.

To determine the net contribution of NO to endothelial-dependent relaxation, cumulative concentration-response curves to ACh were performed in the presence or absence of the NOS inhibitor, L-NAME. L-NAME completely abolished ACh-induced relaxations in all groups (Figures 1B-1E). However, the NO contribution, estimated from the difference between the AUC obtained in arteries pre-incubated or not with L-NAME, was significantly reduced in HF C ($\Delta AUC_{HF C}$ = 121 *vs* $\Delta AUC_{Chow C}$ = 200; p<0.01) mice but preserved by the treatment with C21 ($\Delta AUC_{HF C21}$ = 184; Figure 1F, see NO contribution in white).

3.3. C21 prevents HFD-induced alterations in vascular responses to Ang II

In another set of experiments, we aimed at evaluating the impact of HF-feeding and the effect of C21 in vascular responses to Ang II. With this purpose, we first assessed contractile responses to Ang II (10^{-9}-10^{-6} mol/L) that were significantly enhanced in HF C mice compared with Chow C mice (Figure 2A and Suppl Table 3). However, HF C21 mice exhibited similar values to the Chow C group and significantly lower than the HF C group (Figure 2A and Suppl

Table 3), thus evidencing a protective effect of C21 by preventing the development of alterations in contractile responses to Ang II.

To elucidate whether AT_2, Mas and B_2 receptors are implicated in these responses, we performed cumulative-concentration curves to Ang II in segments previously incubated with the specific antagonists of the AT_2R (PD 123177), the MasR (A779) and the B_2R (HOE-140). As shown in Figures 2B-2E, the preincubation with PD123177, A779 or HOE-140 significantly enhanced Ang II-induced constriction in arteries from all experimental groups (Figures 2B, 2C and 2E) except for the HF C group (Figure 2D), which were unresponsive to the preincubation with any of the three antagonists, as evidenced by E_{max} and AUC values (Suppl Table 3). These data indicate that AT_2, Mas and B_2 receptors are all involved in attenuating contractile responses to Ang II in Chow mice. However, with HF diet the inhibition of the 3 receptors had no effect on vessel contraction, only to be restored when given the HF diet with C21 supplementation. Moreover, although the expression of the AT_1R was significantly enhanced by the HF diet, no differences were detected in the expression of the AT_2R (Suppl. Figure 1). Altogether, these data suggest a lack of functionality of AT_2, Mas and B_2 receptors during obesity that was prevented by the treatment with C21.

To assess the impact of HF feeding and C21 on relaxant responses to Ang II, we performed cumulative-concentration curves to Ang II (10^{-9} to 10^{-6} mol/L) in segments pre-incubated with the AT_1R antagonist, losartan (10^{-7} mol/L), and pre-contracted with Phe (10^{-6} mol/L). Interestingly, Ang II was unable to elicit AT_2R-mediated relaxant responses in HF C mice (Figure 3A and Suppl Table 4) compared with Chow C mice. Nevertheless, when treated with C21, HF mice exhibited a significant relaxant response to Ang II (about 20%, Figure 3A), similar to the Chow C. In addition, preincubation with PD123177, A779 or HOE-140 completely abolished Ang II-induced relaxation in both Chow-fed groups (Figures 3B, 3C) and in HF C21 mice (Figure 3E) but did not modify vascular responses to Ang II in HF C mice

(Figure 3D) as evidenced by the E_{max} values (Suppl Table 4). These results confirm the loss of functionality of AT_2, Mas and B_2 receptors in obesity, that is preserved by the treatment with C21.

3.4. C21 prevents the development of arterial stiffness in HF mice

Mechanical properties were analyzed from the circumferential wall tension-stretch relationship, whose slope represents the β-index, a marker of intrinsic arterial stiffness. As shown in Figure 4A, aorta segments from HF C mice exhibited a shift towards the left in the tension-stretch relationship that was paralleled by a significant increase in the β-index (Figure 4B). This effect was prevented by the treatment with C21. No effect of C21 was observed in Chow animals (Figure 4A and 4B).

To elucidate whether there is a relationship between arterial stiffness and AT_1R activation, the correlation between contractile effect to Ang II evaluated by the E_{max} value and the β-index was measured. Interestingly, with coefficient of correlation of 0.573 ($p<0.001$), a significant positive correlation was observed between the 2 parameters (Figure 4C).

3.5. C21 prevented HF-induced collagen deposition and increased TGF-$β_1$ in abdominal aorta

Differences in collagen deposition was assessed in aorta segments of the 4 groups of mice by means of immunofluorescence (type I and III collagen) and fluorometric assays (total collagen content). HF C mice showed a significant increase in the amount of collagen type I/III (Figures 5A and 5B; Suppl Figure 2) as well as an increase in total collagen levels (Figure 5C). Intriguingly, the stimulation of the AT_2R by C21 in HF mice prevented these alterations (Figures 5A-5C). Moreover, a positive correlation was detected between total collagen levels and AT_1R activation and β-index (Figures 5D and 5E, respectively).

TGF-β_1 concentration was also measured in abdominal aorta segments. Although no significant changes were detected between HF C and Chow C mice, HF C21 mice exhibited lower TGF-β_1 levels compared with HF C mice (Figure 6A; $P<0.05$). In addition, a positive correlation was detected between TGF-β_1 levels and contractile responses to Ang II, total collagen and β-values (Figures 6B, 6C and 6D, respectively).

3.6. C21 prevented the increase of plasma MMP-2 and -9 activities in HF C mice.

Plasma pro-MMP-2, MMP-2 and MMP-9 activities were analyzed by gelatin zymography. Pro-MMP-2 (72 KDa) and active MMP-2 (62 KDa) activities were significantly enhanced in HF C mice together with higher levels of active MMP-9 (82 KDa) compared with Chow C mice (Figures 7A-D). Treatment with C21 prevented these alterations as shown by pro-MMP-2, MMP-2 and MMP-9 activities from HF C21 mice that were similar to the Chow C group (Figure 7A-D). In addition, a positive correlation between MMP-2 and MMP-9 and total collagen levels (Figure 7E and 7F, respectively) as well as a significant positive correlation between MMP-9 activity and contractile responses to Ang II (Figures 7G) were detected.

4. **DISCUSSION**

Endothelial dysfunction has been traditionally considered as the major mechanism responsible for obesity-derived vascular damage[51]. However, vascular remodeling and arterial stiffness have emerged as important additional mechanisms[10, 11], in which AT$_1$R overactivation could play a key role. However, these alterations might have different effects on different vascular beds[19]. Indeed, the increased expression of AT$_1$R detected in the abdominal aorta[52], among other phenotypic and physiologic differences, makes it more susceptible to the development of vascular alterations[53].

To test the hypothesis that AT$_2$R activation could prevent obesity-induced endothelial dysfunction and vascular stiffening, we used a mouse model of diet-induced obesity treated

with C21, a specific AT_2R agonist. The novel findings of this study are that the AT_2R stimulation by C21: i) prevented obesity-related endothelial dysfunction in the abdominal aorta by preserving NO availability and ii) prevented obesity-related arterial stiffening at least partly by inhibiting MMPs activity and TGF-β_1 upregulation which in turn led to ECM remodeling (Figure 8).

The development of obesity-related endothelial dysfunction linked to a compromised NO availability has been reported in humans and rodents[3, 5-8]. In this context, we have recently demonstrated that the pharmacological stimulation of the AT_2R preserves NO availability and endothelial function in the thoracic aorta from HF mice and reduces Ang II-induced contractions[5]. The major difference between these studies lies in regional differences on Ang II-induced contractile capacity which is 10-fold higher in the abdominal aorta than in the thoracic aorta and significantly enhanced by HF feeding. More specifically, whereas E_{max} in abdominal segments from HF animals reached approximately 60% due to an AT_1R overactivation, the thoracic aorta presented a maximal contraction to Ang II of 5%. These results are in accordance with the study performed by Zhou *et al.* showing minimal responses to Ang II in mouse thoracic aorta compared to the abdominal segment, possibly due to the differential expression of AT_1R mRNA levels, that was significantly lower in the thoracic than in the abdominal aorta[52]. Interestingly, the effects of C21 in mitigating Ang II-induced contractions in HF mice was also detected in the abdominal aorta and shown to render even greater protective vascular effect than the previously described in thoracic segments[5]. Moreover, since no changes were detected in the expression of the AT_2R neither with the HF diet nor with the treatment with C21, we might discard that the inability of Ang II to activate the AT_2R in HF mice was due to a reduced expression of this receptor rather than to a lack of functionality, effect that is preserved by the treatment with C21 as recently suggested in our previous study[5].

From a mechanistic point of view, a study performed in human endothelial cells showed that AT$_2$R stimulation does not only enhance eNOS activity and NO release through activating eNOS phosphorylation in Ser[1177] as we have also corroborated[5], but also through dephosphorylating and inactivating Tyr[657] and Thr[495] residues[54].In our model, abdominal aortas from HF C animals did not show any vasodilatory effect in response to Ang II. This may indicate a loss of AT$_2$R functionality, as we previously described in the thoracic aorta[5]. These results are in conflict with others showing increased AT$_2$R expression and AT$_2$R-mediated relaxation in the abdominal aorta from HF-fed rats, although their animals had a shorter exposure to the HF diet[55], suggesting that the AT$_2$R-mediated protective effect could be lost only after a prolonged exposure to HF diets. Importantly, the pharmacological stimulation of AT$_2$R by C21 prevented alterations in both contractile and relaxant responses to Ang II in HF mice, suggesting that C21 contributes to maintain AT$_2$R-mediated beneficial effects. Furthermore, since C21-mediated relaxation was abolished when either the AT$_2$R, the MasR or the B$_2$R was blocked by their specific antagonists, these data suggest that the interaction between the three receptors, previously described in the thoracic aorta[5], is also essential to maintain the protective effects derived from the AT$_2$R activation in the abdominal aorta.

In obesity, a defective ECM remodeling plays a central role in arterial stiffness. Ang II has shown to favor an imbalance in the degradation/synthesis of the ECM components, especially collagen and elastin[56, 57]. In this direction, we detected a significant increase in collagen deposition in segments of abdominal aorta from HF mice, which correlates with Ang II-mediated contraction and arterial stiffness. These results document a crucial role for RAS activation on the development of arterial stiffness, as previously suggested by Eberson et al[58]. It is important to highlight that the collagen/elastin ratio in the abdominal aorta is very high compared with other conductance arteries[29, 53], which is the reason we were unable to detect measurable amounts of elastin in the abdominal aorta. Therefore, the higher density of collagen

present in the abdominal aorta, could make it more susceptible to the development of obesity-induced arterial stiffness than the thoracic aorta[59].

Alterations in ECM composition result from an increased MMP activity or an imbalance between MMPs and their natural inhibitors, the tissue inhibitors of metalloproteinases (TIMPs)[42]. In accordance to the finding that Ang II induces MMPs activation[60-62], the plasma activity of proMMP-2, MMP-2 and MMP-9, considered as the most relevant proteinases involved in the ECM degradation within the aortic wall[63] and overactivated in obese humans[64, 65], was significantly enhanced in HF mice and positively correlated with collagen deposition in our study.

One of the main findings of this study is that AT_2R stimulation by C21 prevented changes in MMP activity and collagen deposition, thus preserving arterial distensibility. In this regard, several studies have suggested an anti-fibrotic effect elicited by AT_2R agonists[66] although its association with MMPs regulation at a vascular level remains to be elucidated. Nevertheless, a study performed in cardiac fibroblasts treated with C21 demonstrated a reduction in MMP-9 activity associated with an increased TIMP-1 activation[67]. Similar effects have been observed in murine models of myocardial infarction[67] or atherosclerosis[68], in which C21 accounted for a reduction of cardiac fibrosis and collagen accumulation as well as a reduction of systemic arterial stiffness linked to a decrease of MMP activation and of TFG-β_1 levels[67].

TGF-β_1 has shown to be the most important profibrotic factor responsible for ECM remodeling due to its ability to induce collagen deposition[32] and favor ECM protein reticulation, thereby accounting for the development of arterial stiffness[69]. Several studies performed in DIO rodents have also provided evidence of an increase of TGF-β_1 in the aorta or the femoral arteries, associated to enhanced collagen accumulation and arterial stiffness[19, 70]. In our model, we were not able to detect a significant increase in TGF-β_1 concentration in the abdominal aorta from HF mice (p=0.07 vs Chow C). However, lower levels of TGF-β_1 were detected in HF C21 mice

compared with HF mice that correlated both with Ang II-induced contractions and β-index. In this direction, several mechanisms that could explain C21-mediated TGF-β_1 reduction have been proposed and include the activation of SMAD/MAPK[71] pathway, the formation of heterodimers between the AT$_2$R and both the AT$_1$R[72] and TGF-β type II receptor[73] and the activation of the eNOS/NO/cGMP[73] axis. Intriguingly, whereas eNOS activation has shown to inhibit TGF-β_1 synthesis[73], acute and chronic NO deficiency have been demonstrated to trigger the activation of MMPs[74, 75]. In light of these observations, we could hypothesize that C21-mediated NO release could also indirectly contribute to preserve ECM composition and arterial elasticity.

In conclusion, this study demonstrates for the first time that AT$_2$R stimulation by C21 not only aids in preventing the development of obesity-derived endothelial dysfunction, but also ECM remodeling and arterial stiffness. Therefore, C21 might constitute a promising therapeutic tool in the prevention of CVD associated to obesity.

Clinical perspectives

- The abdominal aorta exhibits important phenotypic features (i.e, small elastin amounts or high expression of the AT$_1$R) that make it highly susceptible to vascular alterations. Because the stimulation of AT$_2$R by Compound 21 is known to attenuate AT$_1$-mediated vascular effects and prevent fibrotic processes, this study aimed to assess the effect of C21 on obesity-derived vascular alterations in the abdominal aorta.

- This study evidence that AT$_2$R stimulation preserves endothelial function and counterbalance increased AT$_1$R-mediated vascular responses in the abdominal aorta from diet-induced obese mice. Moreover, C21 also averts collagen deposition derived from augmented TGF-β_1 levels and MMP-2/MMP-9 activities, thus preserving vascular elasticity.

- Since the abdominal aorta is highly susceptible to obesity-induced vascular alterations that might ultimately derive in further complications such as aneurysms, among others, associated with high morbi/mortality rates, these data point out the potential of C21 as a promising therapeutic tool in the prevention of obesity-related cardiovascular disorders.

Conflict of interest: none declared.

References

1. Morris MJ. Cardiovascular and metabolic effects of obesity. *Clin Exp Pharmacol Physiol*. 2008;35:416-419
2. Arancibia-Radich J, Gonzalez-Blazquez R, Alcala M, Martin-Ramos M, Viana M, Arribas S, Delporte C, Fernandez-Alfonso MS, Somoza B, Gil-Ortega M. Beneficial effects of murtilla extract and madecassic acid on insulin sensitivity and endothelial function in a model of diet-induced obesity. *Sci Rep*. 2019;9:599
3. Gil-Ortega M, Condezo-Hoyos L, Garcia-Prieto CF, Arribas SM, Gonzalez MC, Aranguez I, Ruiz-Gayo M, Somoza B, Fernandez-Alfonso MS. Imbalance between pro and anti-oxidant mechanisms in perivascular adipose tissue aggravates long-term high-fat diet-derived endothelial dysfunction. *PloS one*. 2014;9:e95312
4. Gil-Ortega M, Martin-Ramos M, Arribas SM, Gonzalez MC, Aranguez I, Ruiz-Gayo M, Somoza B, Fernandez-Alfonso MS. Arterial stiffness is associated with adipokine dysregulation in non-hypertensive obese mice. *Vascular pharmacology*. 2016;77:38-47
5. Gonzalez-Blazquez R, Alcala M, Fernandez-Alfonso MS, Steckelings UM, Lorenzo MP, Viana M, Boisvert WA, Unger T, Gil-Ortega M, Somoza B. C21 preserves endothelial function in the thoracic aorta from dio mice: Role for at2, mas and b2 receptors. *Clinical science*. 2021;135:1145-1163
6. Virdis A, Colucci R, Bernardini N, Blandizzi C, Taddei S, Masi S. Microvascular endothelial dysfunction in human obesity: Role of tnf-alpha. *The Journal of clinical endocrinology and metabolism*. 2019;104:341-348
7. Virdis A, Masi S, Colucci R, Chiriaco M, Uliana M, Puxeddu I, Bernardini N, Blandizzi C, Taddei S. Microvascular endothelial dysfunction in patients with obesity. *Current hypertension reports*. 2019;21:32
8. Garcia-Prieto CF, Hernandez-Nuno F, Rio DD, Ruiz-Hurtado G, Aranguez I, Ruiz-Gayo M, Somoza B, Fernandez-Alfonso MS. High-fat diet induces endothelial dysfunction through a down-regulation of the endothelial ampk-pi3k-akt-enos pathway. *Molecular nutrition & food research*. 2015;59:520-532
9. Li H, Bao Y, Zhang X, Yu Y. Free fatty acids induce endothelial dysfunction and activate protein kinase c and nuclear factor-kappab pathway in rat aorta. *International journal of cardiology*. 2011;152:218-224
10. Masi S, Georgiopoulos G, Chiriaco M, Grassi G, Seravalle G, Savoia C, Volpe M, Taddei S, Rizzoni D, Virdis A. The importance of endothelial dysfunction in resistance artery remodelling and cardiovascular risk. *Cardiovascular research*. 2020;116:429-437
11. Safar ME, Czernichow S, Blacher J. Obesity, arterial stiffness, and cardiovascular risk. *Journal of the American Society of Nephrology : JASN*. 2006;17:S109-111
12. Turin TC, Kita Y, Rumana N, Takashima N, Kadota A, Matsui K, Sugihara H, Morita Y, Nakamura Y, Miura K, Ueshima H. Brachial-ankle pulse wave velocity predicts all-cause mortality in the general population: Findings from the takashima study, japan. *Hypertension research : official journal of the Japanese Society of Hypertension*. 2010;33:922-925
13. Vlachopoulos C, Aznaouridis K, Stefanadis C. Prediction of cardiovascular events and all-cause mortality with arterial stiffness: A systematic review and meta-analysis. *Journal of the American College of Cardiology*. 2010;55:1318-1327
14. Brunner EJ, Shipley MJ, Ahmadi-Abhari S, Tabak AG, McEniery CM, Wilkinson IB, Marmot MG, Singh-Manoux A, Kivimaki M. Adiposity, obesity, and arterial aging: Longitudinal study of aortic stiffness in the whitehall ii cohort. *Hypertension*. 2015;66:294-300

15. Grassi G, Diez J. Obesity-related cardiac and vascular structural alterations: Beyond blood pressure overload. *Journal of hypertension*. 2009;27:1750-1752

16. Kangas P, Tikkakoski AJ, Tahvanainen AM, Leskinen MH, Viitala JM, Kahonen M, Koobi T, Niemela OJ, Mustonen JT, Porsti IH. Metabolic syndrome may be associated with increased arterial stiffness even in the absence of hypertension: A study in 84 cases and 82 controls. *Metabolism: clinical and experimental*. 2013;62:1114-1122

17. Nemes A, Gavaller H, Csajbok E, Forster T, Csanady M. Obesity is associated with aortic enlargement and increased stiffness: An echocardiographic study. *Int J Cardiovasc Imaging*. 2008;24:165-171

18. Sato H, Hayashi J, Harashima K, Shimazu H, Kitamoto K. A population-based study of arterial stiffness index in relation to cardiovascular risk factors. *J Atheroscler Thromb*. 2005;12:175-180

19. Bender SB, Castorena-Gonzalez JA, Garro M, Reyes-Aldasoro CC, Sowers JR, DeMarco VG, Martinez-Lemus LA. Regional variation in arterial stiffening and dysfunction in western diet-induced obesity. *American journal of physiology. Heart and circulatory physiology*. 2015;309:H574-582

20. DeMarco VG, Habibi J, Jia G, Aroor AR, Ramirez-Perez FI, Martinez-Lemus LA, Bender SB, Garro M, Hayden MR, Sun Z, Meininger GA, Manrique C, Whaley-Connell A, Sowers JR. Low-dose mineralocorticoid receptor blockade prevents western diet-induced arterial stiffening in female mice. *Hypertension*. 2015;66:99-107

21. Sista AK, O'Connell MK, Hinohara T, Oommen SS, Fenster BE, Glassford AJ, Schwartz EA, Taylor CA, Reaven GM, Tsao PS. Increased aortic stiffness in the insulin-resistant zucker fa/fa rat. *American journal of physiology. Heart and circulatory physiology*. 2005;289:H845-851

22. Dobrin PB. Mechanical properties of arterises. *Physiological reviews*. 1978;58:397-460

23. Bouissou C, Lacolley P, Dabire H, Safar ME, Gabella G, Duchatelle V, Challande P, Bezie Y. Increased stiffness and cell-matrix interactions of abdominal aorta in two experimental nonhypertensive models: Long-term chemically sympathectomized and sinoaortic denervated rats. *Journal of hypertension*. 2014;32:652-658

24. Sehgel NL, Zhu Y, Sun Z, Trzeciakowski JP, Hong Z, Hunter WC, Vatner DE, Meininger GA, Vatner SF. Increased vascular smooth muscle cell stiffness: A novel mechanism for aortic stiffness in hypertension. *American journal of physiology. Heart and circulatory physiology*. 2013;305:H1281-1287

25. Spinale FG. Myocardial matrix remodeling and the matrix metalloproteinases: Influence on cardiac form and function. *Physiological reviews*. 2007;87:1285-1342

26. Basalyga DM, Simionescu DT, Xiong W, Baxter BT, Starcher BC, Vyavahare NR. Elastin degradation and calcification in an abdominal aorta injury model: Role of matrix metalloproteinases. *Circulation*. 2004;110:3480-3487

27. Ceron CS, Rizzi E, Guimaraes DA, Martins-Oliveira A, Cau SB, Ramos J, Gerlach RF, Tanus-Santos JE. Time course involvement of matrix metalloproteinases in the vascular alterations of renovascular hypertension. *Matrix Biol*. 2012;31:261-270

28. Wolinsky H. Comparison of medial growth of human thoracic and abdominal aortas. *Circulation research*. 1970;27:531-538

29. Wolinsky H, Glagov S. Comparison of abdominal and thoracic aortic medial structure in mammals. Deviation of man from the usual pattern. *Circulation research*. 1969;25:677-686

30. Dobrin PB. Pathophysiology and pathogenesis of aortic aneurysms. Current concepts. *Surg Clin North Am*. 1989;69:687-703

31. He CM, Roach MR. The composition and mechanical properties of abdominal aortic aneurysms. *J Vasc Surg*. 1994;20:6-13

32. Leask A, Abraham DJ. Tgf-beta signaling and the fibrotic response. *FASEB journal : official publication of the Federation of American Societies for Experimental Biology*. 2004;18:816-827

33. Annes JP, Munger JS, Rifkin DB. Making sense of latent tgfbeta activation. *J Cell Sci*. 2003;116:217-224

34. Glenn DJ, Cardema MC, Ni W, Zhang Y, Yeghiazarians Y, Grapov D, Fiehn O, Gardner DG. Cardiac steatosis potentiates angiotensin ii effects in the heart. *American journal of physiology. Heart and circulatory physiology*. 2015;308:H339-350

35. Ruiz-Ortega M, Rodriguez-Vita J, Sanchez-Lopez E, Carvajal G, Egido J. Tgf-beta signaling in vascular fibrosis. *Cardiovascular research*. 2007;74:196-206

36. Chen Q, Jin M, Yang F, Zhu J, Xiao Q, Zhang L. Matrix metalloproteinases: Inflammatory regulators of cell behaviors in vascular formation and remodeling. *Mediators Inflamm*. 2013;2013:928315

37. Rehman A, Rahman AR, Rasool AH. Effect of angiotensin ii on pulse wave velocity in humans is mediated through angiotensin ii type 1 (at(1)) receptors. *Journal of human hypertension*. 2002;16:261-266

38. Yiannikouris F, Gupte M, Putnam K, Thatcher S, Charnigo R, Rateri DL, Daugherty A, Cassis LA. Adipocyte deficiency of angiotensinogen prevents obesity-induced hypertension in male mice. *Hypertension*. 2012;60:1524-1530

39. Abadir PM, Periasamy A, Carey RM, Siragy HM. Angiotensin ii type 2 receptor-bradykinin b2 receptor functional heterodimerization. *Hypertension*. 2006;48:316-322

40. Jones ES, Black MJ, Widdop RE. Influence of angiotensin ii subtype 2 receptor (at(2)r) antagonist, pd123319, on cardiovascular remodelling of aged spontaneously hypertensive rats during chronic angiotensin ii subtype 1 receptor (at(1)r) blockade. *International journal of hypertension*. 2012;2012:543062

41. Tschope C, Westermann D, Dhayat N, Dhayat S, Altmann C, Steendijk P, Schultheiss HP, Walther T. Angiotensin at2 receptor deficiency after myocardial infarction: Its effects on cardiac function and fibrosis depend on the stimulus. *Cell biochemistry and biophysics*. 2005;43:45-52

42. Brassard P, Amiri F, Schiffrin EL. Combined angiotensin ii type 1 and type 2 receptor blockade on vascular remodeling and matrix metalloproteinases in resistance arteries. *Hypertension*. 2005;46:598-606

43. Dandapat A, Hu CP, Chen J, Liu Y, Khan JA, Remeo F, Carey RM, Hermonat PL, Mehta JL. Over-expression of angiotensin ii type 2 receptor (agtr2) decreases collagen accumulation in atherosclerotic plaque. *Biochemical and biophysical research communications*. 2008;366:871-877

44. Gonzalez-Blazquez R, Somoza B, Gil-Ortega M, Martin Ramos M, Ramiro-Cortijo D, Vega-Martin E, Schulz A, Ruilope LM, Kolkhof P, Kreutz R, Fernandez-Alfonso MS. Finerenone attenuates endothelial dysfunction and albuminuria in a chronic kidney disease model by a reduction in oxidative stress. *Front Pharmacol*. 2018;9:1131

45. Angus JA, Wright CE. Techniques to study the pharmacodynamics of isolated large and small blood vessels. *J Pharmacol Toxicol Methods*. 2000;44:395-407

46. Gutierrez-Arzapalo PY, Rodriguez-Rodriguez P, Ramiro-Cortijo D, Lopez de Pablo AL, Lopez-Gimenez MR, Condezo-Hoyos L, Greenwald SE, Gonzalez MDC, Arribas SM. Role of fetal nutrient restriction and postnatal catch-up growth on structural and mechanical alterations of rat aorta. *The Journal of physiology*. 2018;596:5791-5806

47. Pfaffl MW. A new mathematical model for relative quantification in real-time rt-pcr. *Nucleic Acids Res*. 2001;29:e45

48. Gil-Ortega M, Garcia-Prieto CF, Ruiz-Hurtado G, Steireif C, Gonzalez MC, Schulz A, Kreutz R, Fernandez-Alfonso MS, Arribas S, Somoza B. Genetic predisposition to

albuminuria is associated with increased arterial stiffness: Role of elastin. *British journal of pharmacology*. 2015;172:4406-4418

49. Briones AM, Gonzalez JM, Somoza B, Giraldo J, Daly CJ, Vila E, Gonzalez MC, McGrath JC, Arribas SM. Role of elastin in spontaneously hypertensive rat small mesenteric artery remodelling. *The Journal of physiology*. 2003;552:185-195

50. Boesby L, Elung-Jensen T, Strandgaard S, Kamper AL. Eplerenone attenuates pulse wave reflection in chronic kidney disease stage 3-4--a randomized controlled study. *PloS one*. 2013;8:e64549

51. Avogaro A, de Kreutzenberg SV. Mechanisms of endothelial dysfunction in obesity. *Clin Chim Acta*. 2005;360:9-26

52. Zhou Y, Dirksen WP, Babu GJ, Periasamy M. Differential vasoconstrictions induced by angiotensin ii: Role of at1 and at2 receptors in isolated c57bl/6j mouse blood vessels. *American journal of physiology. Heart and circulatory physiology*. 2003;285:H2797-2803

53. Halloran BG, Davis VA, McManus BM, Lynch TG, Baxter BT. Localization of aortic disease is associated with intrinsic differences in aortic structure. *The Journal of surgical research*. 1995;59:17-22

54. Peluso AA, Bertelsen JB, Andersen K, Mortsensen TP, Hansen PB, Sumners C, Bader M, Santos RA, Steckelings UM. Identification of protein phosphatase involvement in the at2 receptor-induced activation of endothelial nitric oxide synthase. *Clinical science*. 2018;132:777-790

55. Karpe PA, Gupta J, Marthong RF, Ramarao P, Tikoo K. Insulin resistance induces a segmental difference in thoracic and abdominal aorta: Differential expression of at1 and at2 receptors. *Journal of hypertension*. 2012;30:132-146

56. Dab H, Hachani R, Dhaouadi N, Sakly M, Hodroj W, Randon J, Bricca G, Kacem K. Regulation of aortic extracellular matrix synthesis via noradrenergic system and angiotensin ii in juvenile rats. *Pharm Biol*. 2012;50:1219-1225

57. Che ZQ, Gao PJ, Shen WL, Fan CL, Liu JJ, Zhu DL. Angiotensin ii-stimulated collagen synthesis in aortic adventitial fibroblasts is mediated by connective tissue growth factor. *Hypertension research : official journal of the Japanese Society of Hypertension*. 2008;31:1233-1240

58. Eberson LS, Sanchez PA, Majeed BA, Tawinwung S, Secomb TW, Larson DF. Effect of lysyl oxidase inhibition on angiotensin ii-induced arterial hypertension, remodeling, and stiffness. *PloS one*. 2015;10:e0124013

59. Zhang J, Zhao X, Vatner DE, McNulty T, Bishop S, Sun Z, Shen YT, Chen L, Meininger GA, Vatner SF. Extracellular matrix disarray as a mechanism for greater abdominal versus thoracic aortic stiffness with aging in primates. *Arteriosclerosis, thrombosis, and vascular biology*. 2016;36:700-706

60. Odenbach J, Wang X, Cooper S, Chow FL, Oka T, Lopaschuk G, Kassiri Z, Fernandez-Patron C. Mmp-2 mediates angiotensin ii-induced hypertension under the transcriptional control of mmp-7 and tace. *Hypertension*. 2011;57:123-130

61. Ruddy JM, Jones JA, Ikonomidis JS. Pathophysiology of thoracic aortic aneurysm (taa): Is it not one uniform aorta? Role of embryologic origin. *Prog Cardiovasc Dis*. 2013;56:68-73

62. Touyz RM. Intracellular mechanisms involved in vascular remodelling of resistance arteries in hypertension: Role of angiotensin ii. *Experimental physiology*. 2005;90:449-455

63. Freestone T, Turner RJ, Coady A, Higman DJ, Greenhalgh RM, Powell JT. Inflammation and matrix metalloproteinases in the enlarging abdominal aortic aneurysm. *Arteriosclerosis, thrombosis, and vascular biology*. 1995;15:1145-1151

64. Andrade VL, Petruceli E, Belo VA, Andrade-Fernandes CM, Caetano Russi CV, Bosco AA, Tanus-Santos JE, Sandrim VC. Evaluation of plasmatic mmp-8, mmp-9, timp-1 and mpo levels in obese and lean women. *Clin Biochem*. 2012;45:412-415

65. Derosa G, Ferrari I, D'Angelo A, Tinelli C, Salvadeo SA, Ciccarelli L, Piccinni MN, Gravina A, Ramondetti F, Maffioli P, Cicero AF. Matrix metalloproteinase-2 and -9 levels in obese patients. *Endothelium*. 2008;15:219-224

66. Steckelings UM, Rompe F, Kaschina E, Namsolleck P, Grzesiak A, Funke-Kaiser H, Bader M, Unger T. The past, present and future of angiotensin ii type 2 receptor stimulation. *Journal of the renin-angiotensin-aldosterone system : JRAAS*. 2010;11:67-73

67. Lauer D, Slavic S, Sommerfeld M, Thone-Reineke C, Sharkovska Y, Hallberg A, Dahlof B, Kintscher U, Unger T, Steckelings UM, Kaschina E. Angiotensin type 2 receptor stimulation ameliorates left ventricular fibrosis and dysfunction via regulation of tissue inhibitor of matrix metalloproteinase 1/matrix metalloproteinase 9 axis and transforming growth factor beta1 in the rat heart. *Hypertension*. 2014;63:e60-67

68. Kljajic ST, Widdop RE, Vinh A, Welungoda I, Bosnyak S, Jones ES, Gaspari TA. Direct at(2) receptor stimulation is athero-protective and stabilizes plaque in apolipoprotein e-deficient mice. *International journal of cardiology*. 2013;169:281-287

69. Foote CA, Castorena-Gonzalez JA, Ramirez-Perez FI, Jia G, Hill MA, Reyes-Aldasoro CC, Sowers JR, Martinez-Lemus LA. Arterial stiffening in western diet-fed mice is associated with increased vascular elastin, transforming growth factor-beta, and plasma neuraminidase. *Frontiers in physiology*. 2016;7:285

70. Martinez-Martinez E, Jurado-Lopez R, Valero-Munoz M, Bartolome MV, Ballesteros S, Luaces M, Briones AM, Lopez-Andres N, Miana M, Cachofeiro V. Leptin induces cardiac fibrosis through galectin-3, mtor and oxidative stress: Potential role in obesity. *Journal of hypertension*. 2014;32:1104-1114; discussion 1114

71. Murphy AM, Wong AL, Bezuhly M. Modulation of angiotensin ii signaling in the prevention of fibrosis. *Fibrogenesis Tissue Repair*. 2015;8:7

72. AbdAlla S, Lother H, Abdel-tawab AM, Quitterer U. The angiotensin ii at2 receptor is an at1 receptor antagonist. *The Journal of biological chemistry*. 2001;276:39721-39726

73. Guo HL, Liao XH, Liu Q, Zhang L. Angiotensin ii type 2 receptor decreases transforming growth factor-beta type ii receptor expression and function in human renal proximal tubule cells. *PloS one*. 2016;11:e0148696

74. Kundu S, Kumar M, Sen U, Mishra PK, Tyagi N, Metreveli N, Lominadze D, Rodriguez W, Tyagi SC. Nitrotyrosinylation, remodeling and endothelial-myocyte uncoupling in inos, cystathionine beta synthase (cbs) knockouts and inos/cbs double knockout mice. *J Cell Biochem*. 2009;106:119-126

75. Tyagi SC, Ratajska A, Weber KT. Myocardial matrix metalloproteinase(s): Localization and activation. *Molecular and cellular biochemistry*. 1993;126:49-59

FIGURE LEGENDS

Figure 1. **Effect of C21 on the obesity-induced endothelial dysfunction in the abdominal aorta.** Cumulative concentration-response curves to ACh (10^{-9}-10^{-4} mol/L) were measured in 2 mm long abdominal aortic segments pre-constricted with Phe (1 µmol/L). Data are expressed relative to the contractile effect exerted by Phe and represented as the mean ± S.E.M. (A) Relaxant responses to ACh from Chow and HF animals treated or not with C21. ***p<0.001 compared with Chow C mice; [#]p<0.05 compared with HF C mice (n = 10). The contribution of NO to the vasorelaxant effects was measured in abdominal aortic segments, pre-incubated or not with L-NAME (10^{-4} mol/L), from (B) Chow C, (C) Chow C21, (D) HF C and (E) HF C21 animals. ***p<0.001 compared with their corresponding matched control groups (n = 5-6). (F) Area under concentration–response curves (AUC) elicited by ACh in the presence (grey bars) or absence (full bar) of L-NAME. AUC is expressed in arbitrary units. White bars represent the difference between the AUC in presence and absence of L-NAME. **p<0.01 (n = 5-6). 2-ANOVA; Tukey's multiple comparisons test.

Figure 2: Role of AT$_2$R, B$_2$R and MasR in the contractile responses to Ang II in the abdominal aorta. Cumulative contractile concentration-response curves to Ang II (10^{-9}-10^{-6} mol/L) were measured in 2 mm long abdominal aortic segments. Contractile data are expressed relative to the maximal contractile effect exerted by KCl (60 mmol/L) and represented as mean ± S.E.M. (A) Contractile responses to Ang II from Chow and HF animals treated or not with C21. ***p<0.001 compared with Chow C mice; [##]p<0.01 compared with HF C mice (n = 10). (B-E) The contribution of AT$_2$R, B$_2$R and MasR to the contractile responses to Ang II was measured in aortic rings from each group, pre-incubated or not with PD123177, A-779 or HOE-140. *p<0.05 and **p<0.01 PD123177 *vs* C; [#]p<0.05 and [###]p<0.001 A779 *vs* C; and [&]p<0.05, [&&]p<0.01 and [&&&]p<0.001 HOE-140 *vs* C (n = 5-7). 2-ANOVA; Tukey's multiple comparisons test.

Figure 3: Role of AT$_2$R, B$_2$R and MasR in the relaxant responses to Ang II in the abdominal aorta. Cumulative relaxant concentration-response curves to Ang II (10^{-9}-10^{-6} mol/L) were measured in 2 mm long abdominal aortic segments pre-contracted with a submaximal concentration of Phe (1 µmol/L) and preincubated with losartan (10^{-7} mol/L). Relaxant data are expressed relative to the contractile effect exerted by Phe and represented as mean ± S.E.M. (A) Relaxant responses to Ang II from Chow and HF animals treated or not with C21. ***$p < 0.001$ compared with Chow C mice; ###$p < 0.001$ compared with HF C mice (n = 10). (B-E) The contribution of AT$_2$R, B$_2$R and MasR to the contractile responses was measured in Phe-precontracted aortic rings from each group, pre-incubated or not with PD123177, A-779 or HOE-140. *$p < 0.05$, **$p < 0.01$ and ***$p < 0.001$ PD123177 *vs* C; #$p < 0.05$, ##$p < 0.01$ and ###$p < 0.001$ A779 *vs* C; and &$p < 0.05$ and &&$p < 0.01$ HOE-140 *vs* C (n = 7). 2-ANOVA; Tukey's multiple comparisons test.

Figure 4: Indicators of arterial stiffness in aortic segments. (A) Circumferential wall tension-stretch relationship in segments of abdominal aorta. (B) Scatter plot with bar graph showing β-values obtained from the slope of the tension-stretch relationship. Data are expressed as mean ± S.E.M. (n = 7-9). **$p < 0.01$ (2-ANOVA; Tukey's multiple comparisons test). (C) Pearson´s correlation between β-index and contractile responses to Ang II (E$_{max}$). Chow C: Black circles; Chow C21: white circles; HF C: black triangles and HF C21 white triangles.

Figure 5. Extracellular matrix remodelling in aortic segments. (A) Representative confocal images showing collagen in segments of abdominal aorta. Vessels were labeled with anti-collagen I/III for type I and III collagen (red). Projections were obtained from serial optical sections captured with a fluorescence confocal microscope (x63 objective, zoom 2). (B) Quantification of type I/III collagen mean fluorescence from confocal images. (C) Total collagen levels quantified by an enzymatic fluorimetry assay. Data are expressed as mean ± S.E.M (n = 5). **$p < 0.01$ and ***$p < 0.001$ (2-ANOVA, Tukey's multiple comparisons test). (D)

Pearson´s correlations between either contractile response to Ang II (E_{max}) or (E) total collagen levels and β-index. Chow C: Black circles; Chow C21: white circles; HF C: black triangles and HF C21 white triangles.

Figure 6: TGF-β₁-related arterial stiffness in aortic segments. (A) Quantification of TGF-β₁ levels in abdominal aorta segments. Results are expressed as mean ± S.E.M (n = 6-7). *p<0.05 (2-ANOVA; Tukey's multiple comparisons test). (B) Pearson´s correlations between TGF-β₁ and contractile responses to Ang II (E_{max}), (C) TGF-β₁ and β-index and (D) TGF-β₁ and total collagen levels. Chow C: Black circles; Chow C21: white circles; HF C: black triangles and HF C21 white triangles.

Figure 7: Matrix metalloproteinases involved in extracellular remodeling in aortic segments. (A) Representative gelatinase zymography images and scatter-plot bar graphs showing quantification of (B) Pro-MMP-2 (72 kDa), (C) MMP-2 (62 kDa) and (D) MMP-9 (82 kDa) activity in plasma samples. Activity data are expressed as % of controls (mean ± S.E.M; n = 6-9). *p<0.05, **p<0.01 (2-ANOVA, Tukey´s multiple comparison test). (E) Pearson´s correlations between total collagen and MMP-2 or (F) total collagen and MMP-9 activities and (G) between contractile responses to Ang II (E_{max}) and MMP-9 activity. Chow C: Black circles; Chow C21: white circles; HF C: black triangles and HF C21 white triangles.

Figure 8: Vascular protection elicited by the treatment with C21 in the abdominal aorta from animals fed a high-fat diet.

The treatment with C21 protects endothelial function by preserving the activity of the axis AT_2R/MasR/B_2R and, consequently, NO release. C21 also prevents ECM remodeling and arterial stiffness by reducing MMPs activity, collagen deposition and TFG-β₁ levels. C21: Compound 21; MMPs: matrix metalloproteinases; NO: nitric oxide; TFG-β₁: transforming

growth factor-beta 1; AT_2R: angiotensin II type II receptor; B_2R: bradykinin type II receptor;

MasR: Mas receptor.

Figure 1
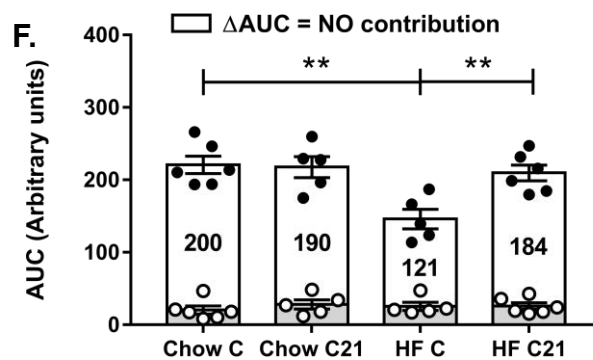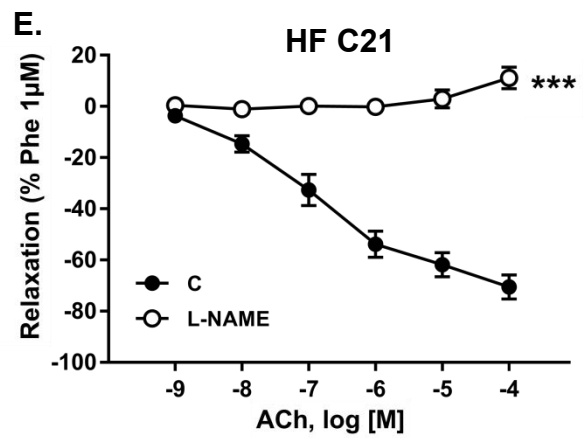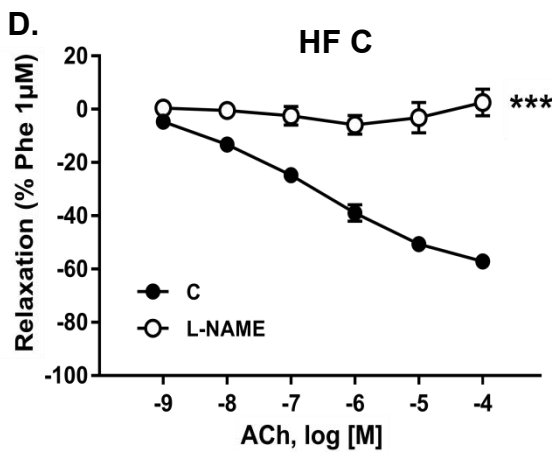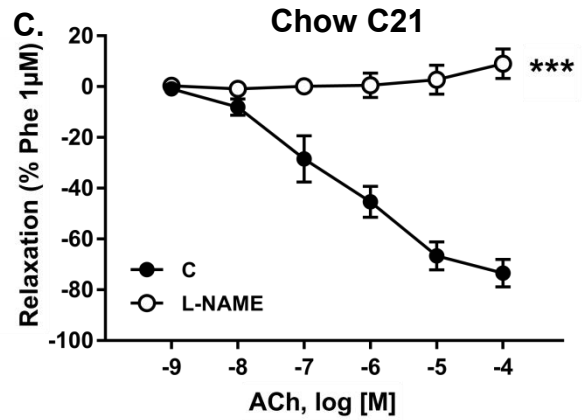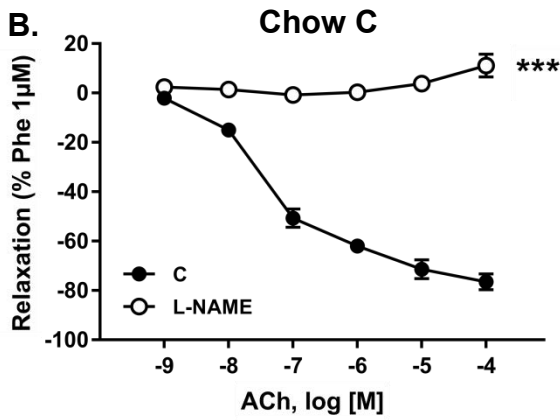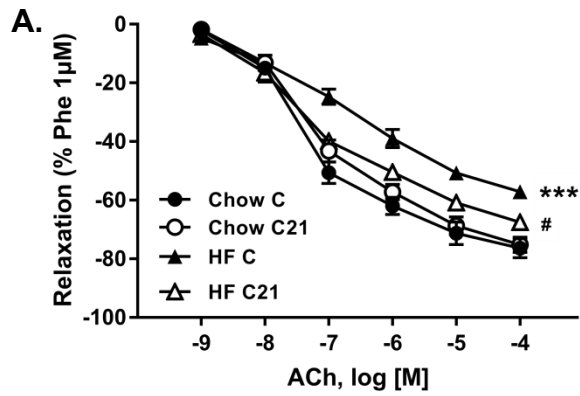
Figure 2
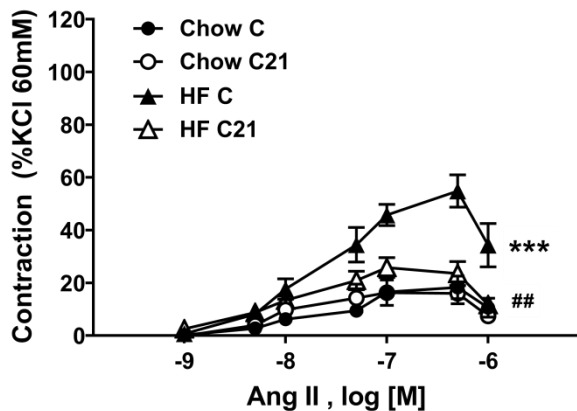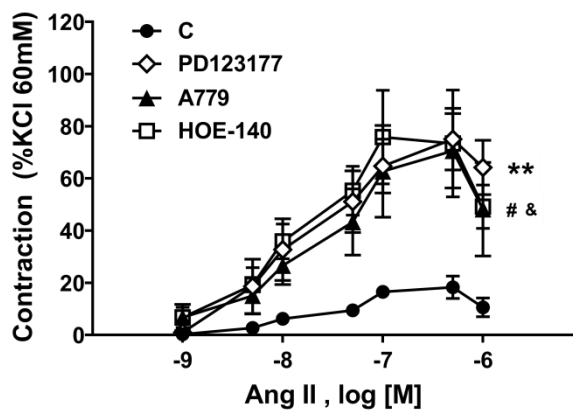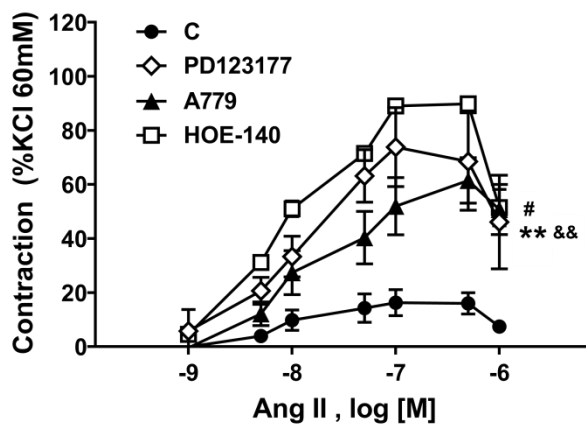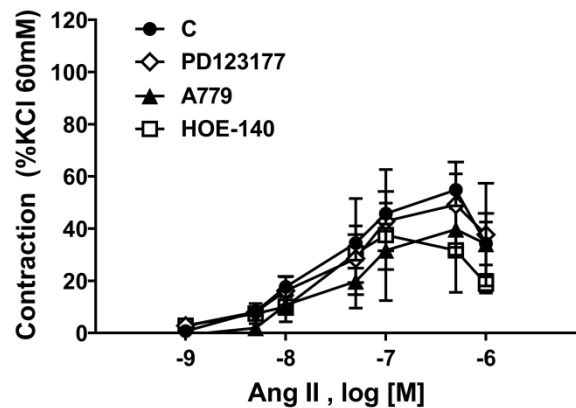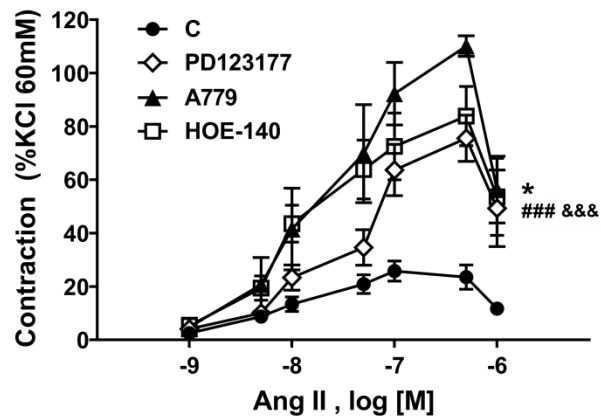
Figure 3

Figure 4

Figure 5

A.

Chow C · Chow C21 · HF C · HF C21 — 25 μm

B.

Type I and III collagen levels (Fluorescence intensity, AU)

*** ***

Chow C   Chow C21   HF C   HF C21

C.

Total collagen levels (μg/mg protein)

** ***

Chow C   Chow C21   HF C   HF C21

D.

r = 0.54
p < 0.05

Contraction to Ang II (E$_{max}$)

Total Collagen levels (μg/mg protein)

- Chow C
- Chow C21
- HF C
- HF C21

E.

r = 0.56
p < 0.05

β-index

Total Collagen levels (μg/mg protein)
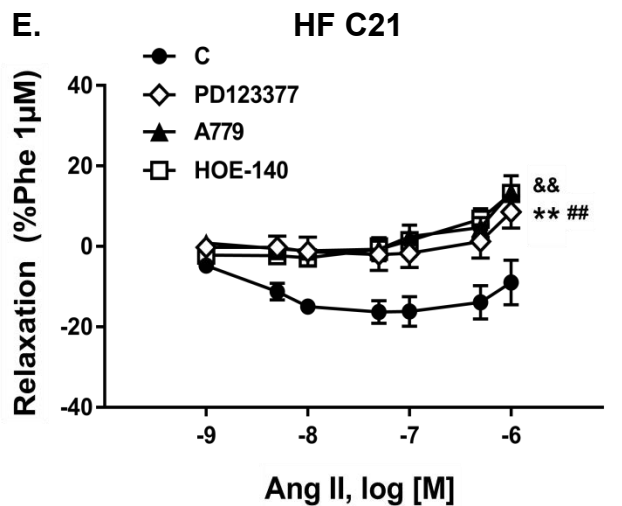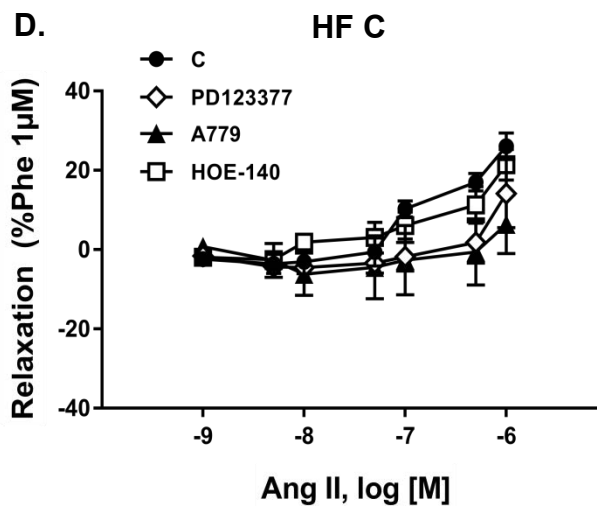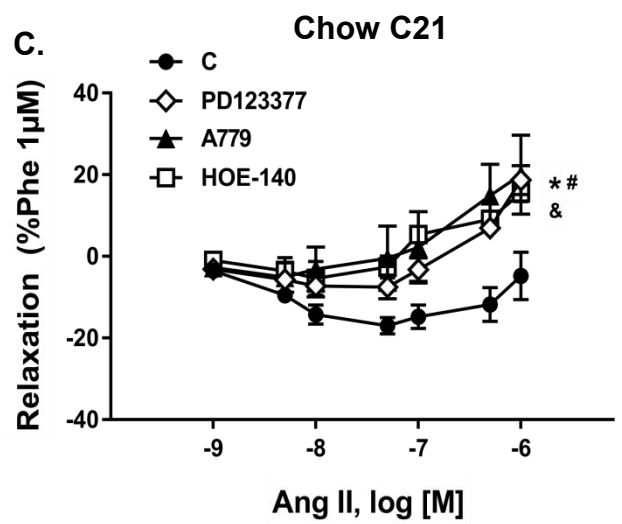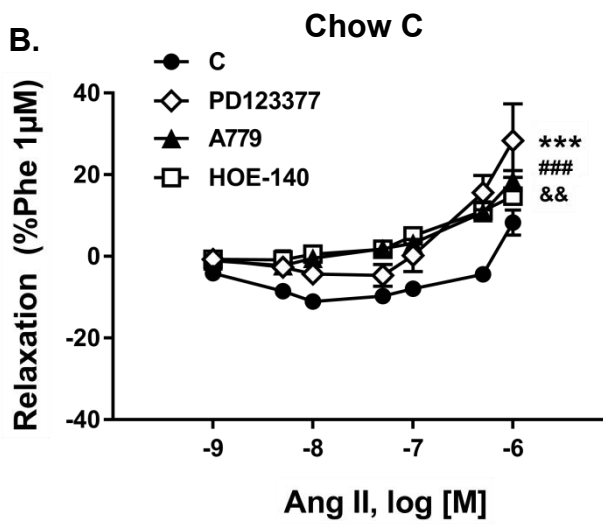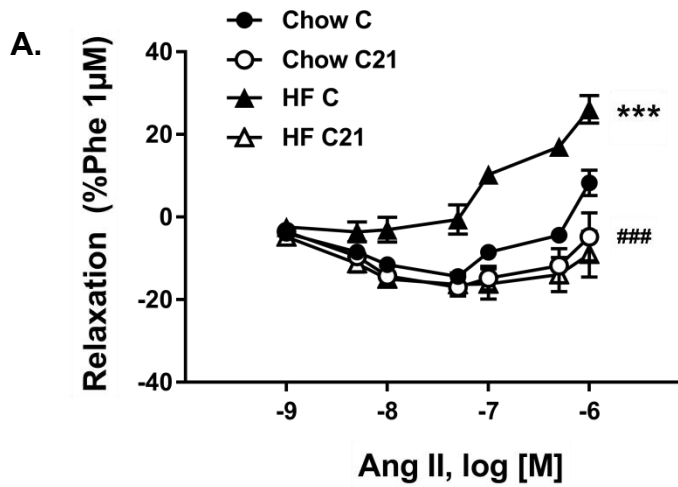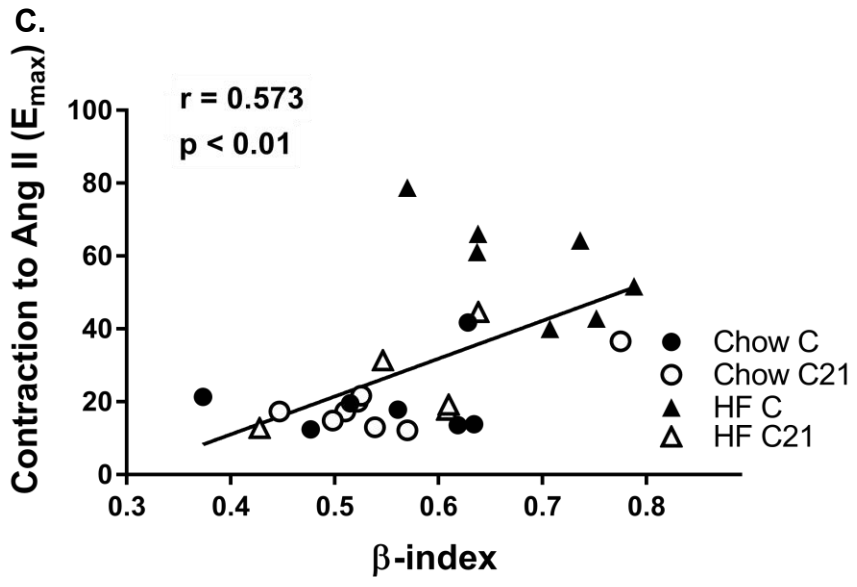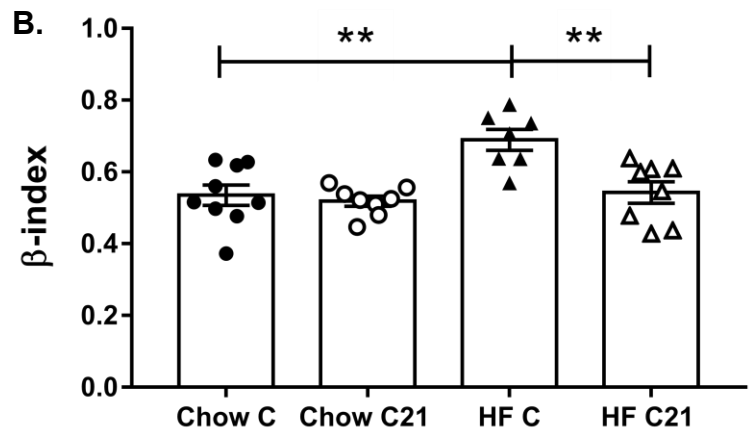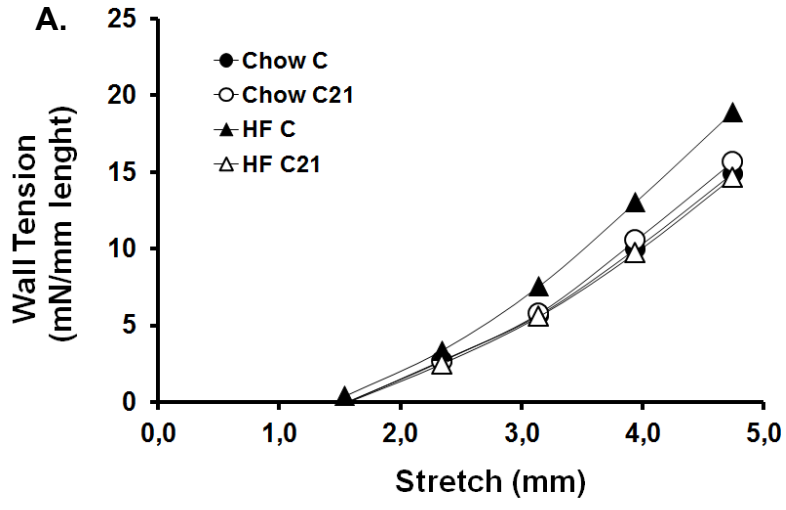
- Chow C
- Chow C21
- HF C
- HF C21
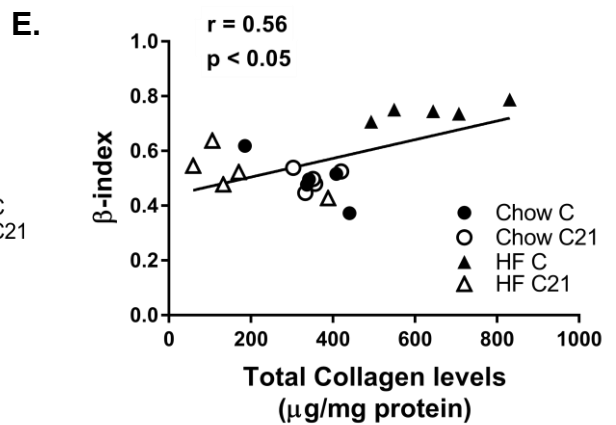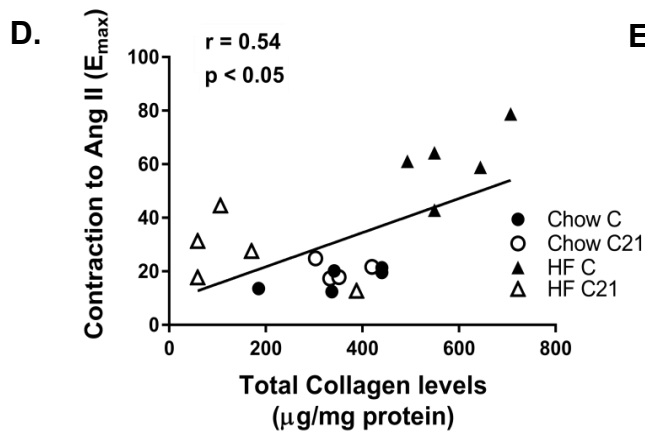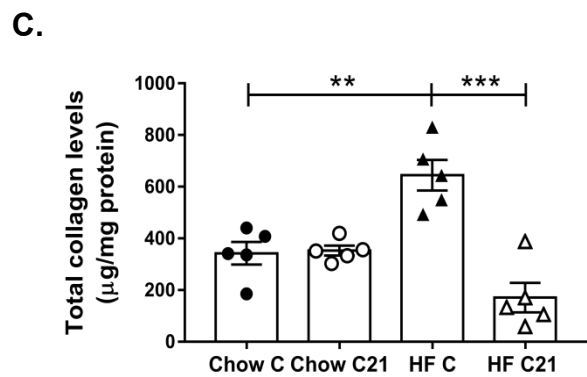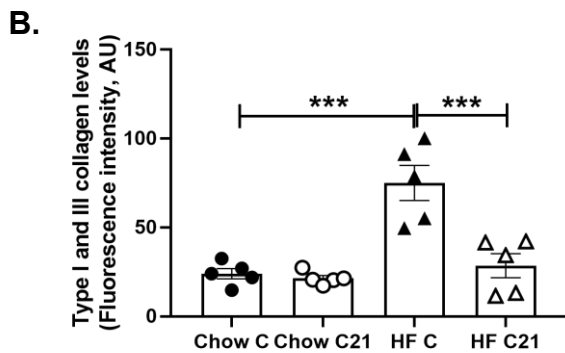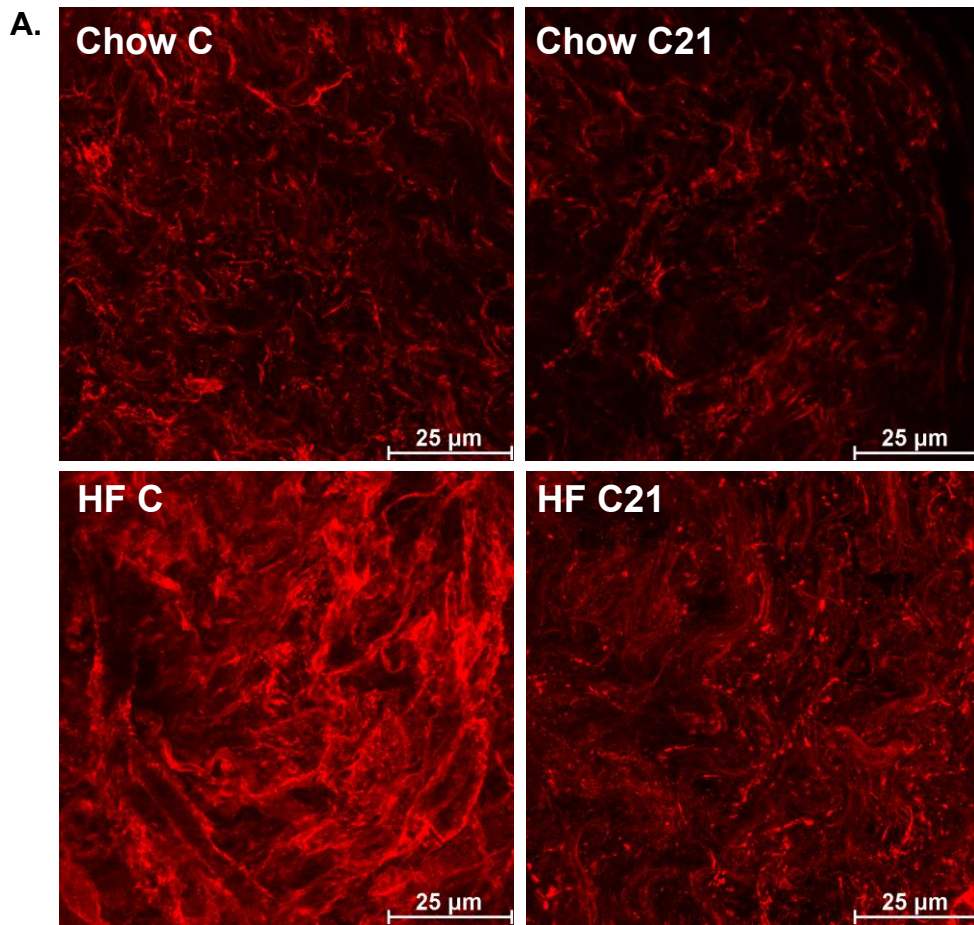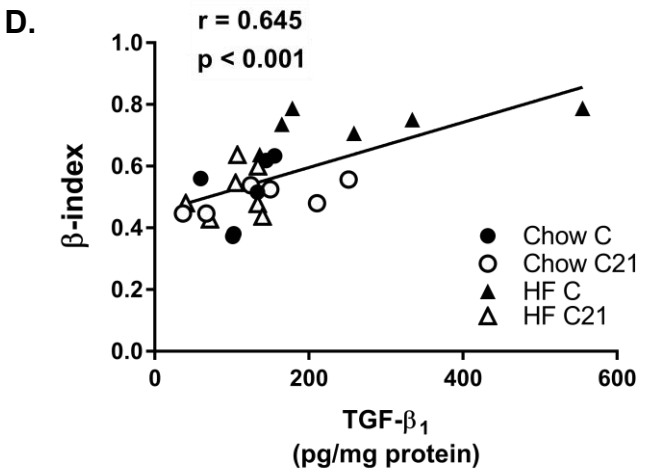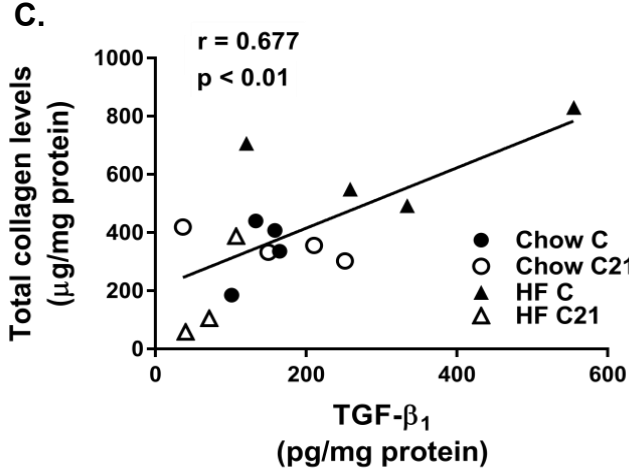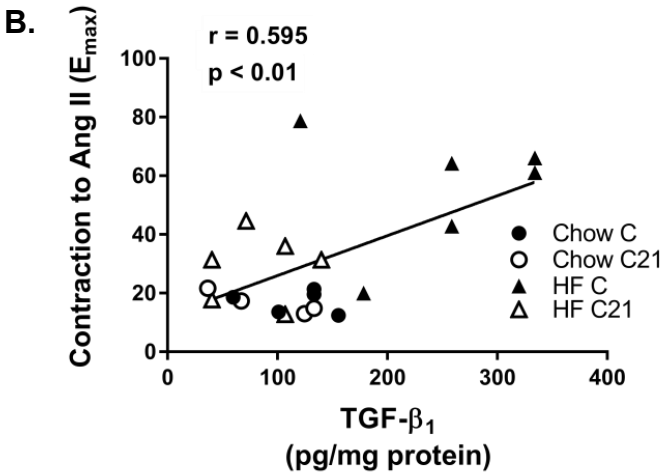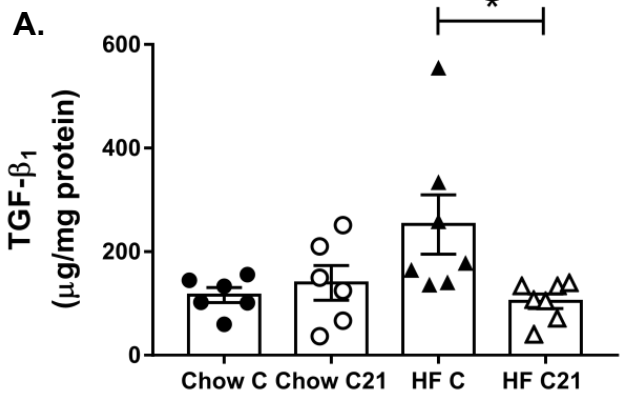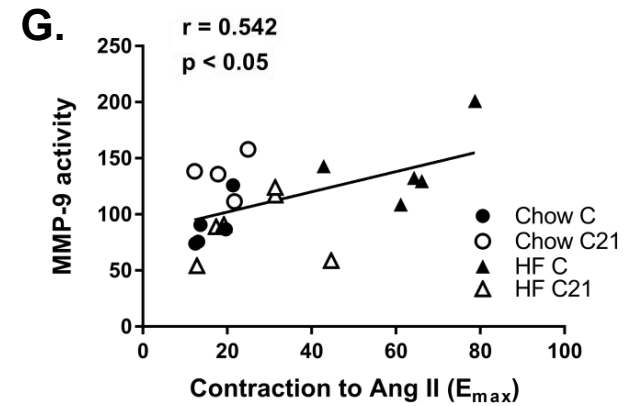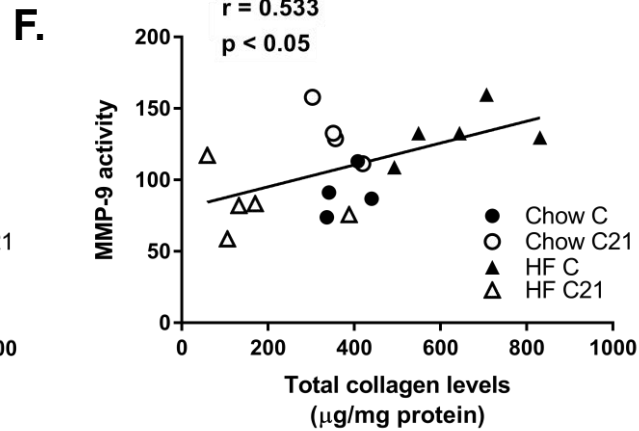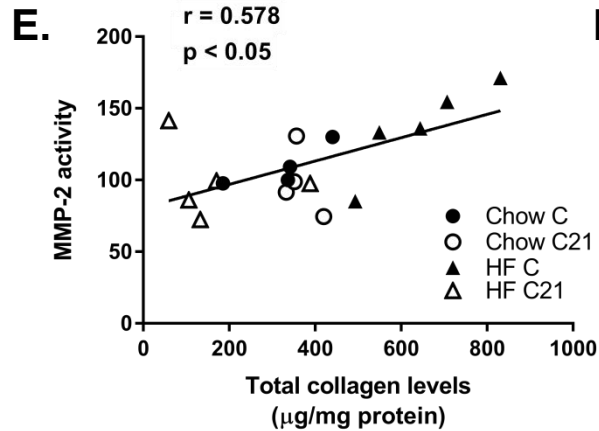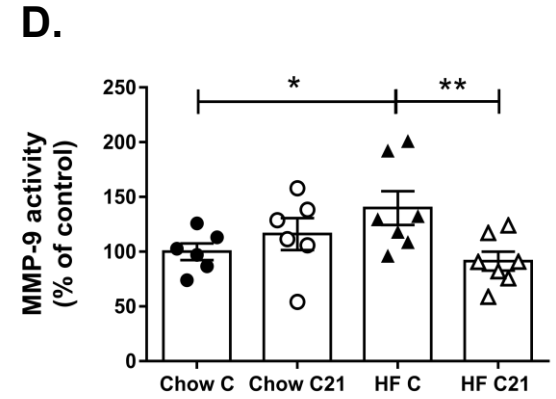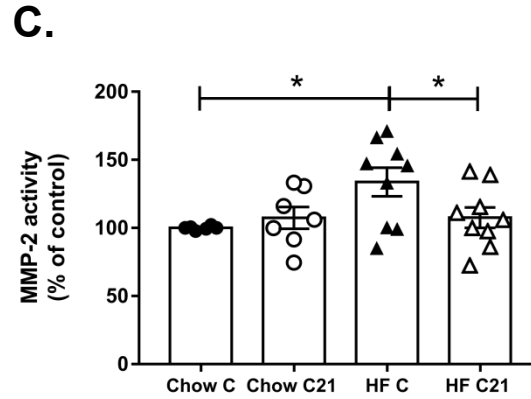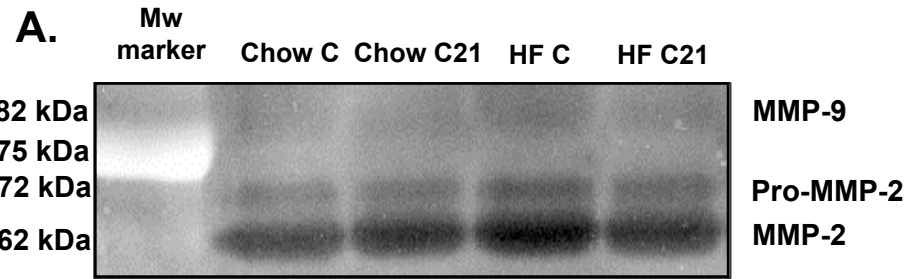
Figure 6

Figure 7

Figure 8
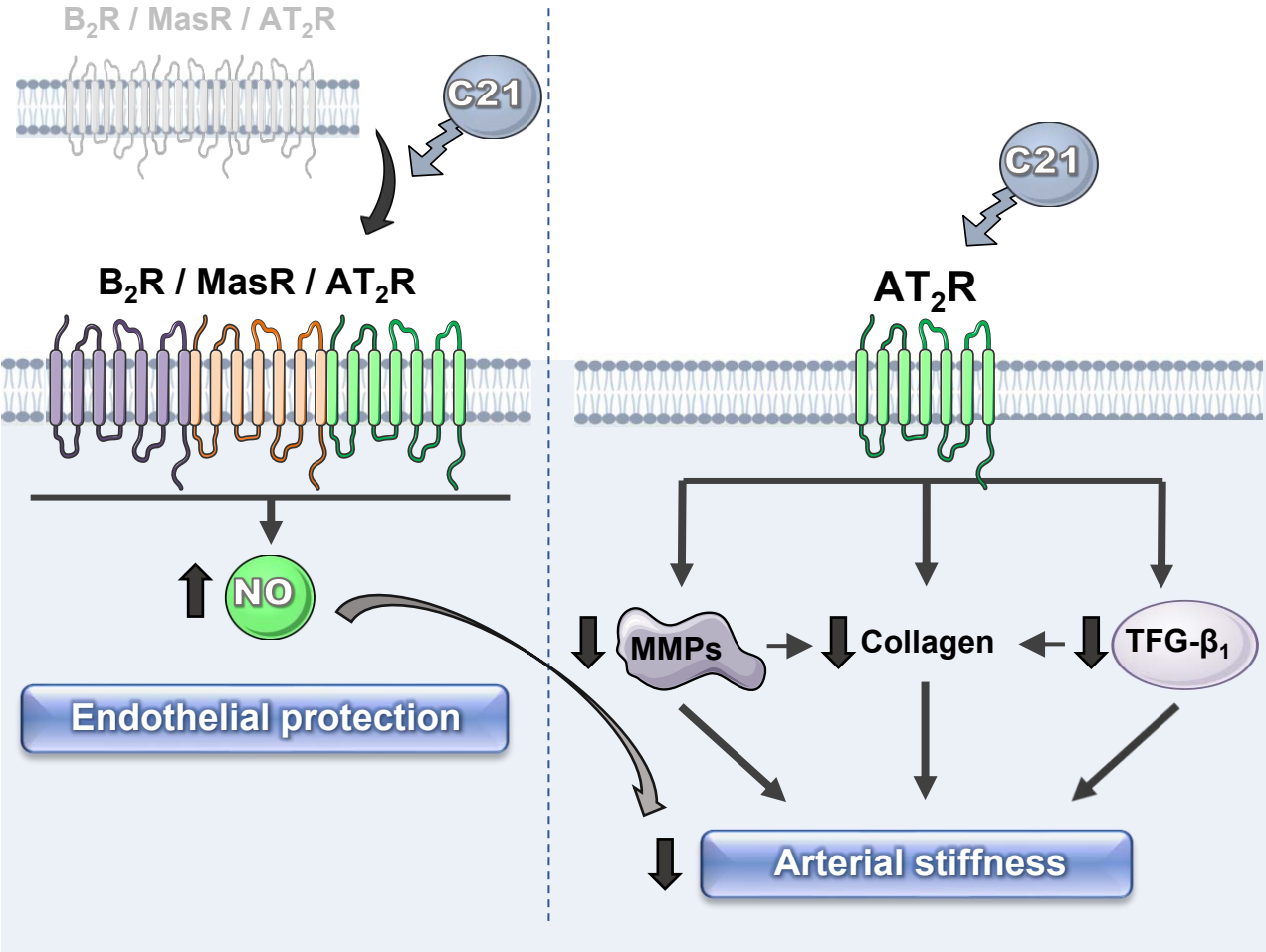
Table 1. Effect of HF-feeding and C21 treatment on BW and food intake.

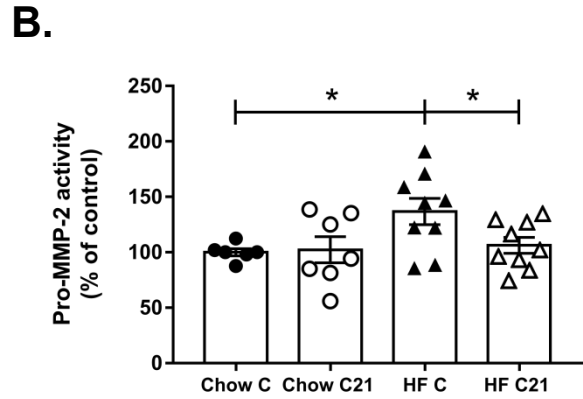|	Chow C	Chow C21	HF C	HF C21
BW increase (g)	6.5 ± 0.6	6.0 ± 0.3	12.4 ± 1.3***	12.8 ± 1.0
Energy Intake (Kcal/mice/day)	7.6 ± 0.1	7.3 ± 0.1	9.8 ± 0.1***	10.4 ± 0.3
Water Intake (mL/day)	3.9 ± 0.1	3.7 ± 0.1	3.3 ± 0.1***	3.1 ± 0.1

Data are expressed as mean $\pm$ SEM (n $= 10$ determinations per group). ***$p<0.001$ *vs* Chow C mice (2-ANOVA; Tukey´s post hoc test).

Supplemental Figure 1
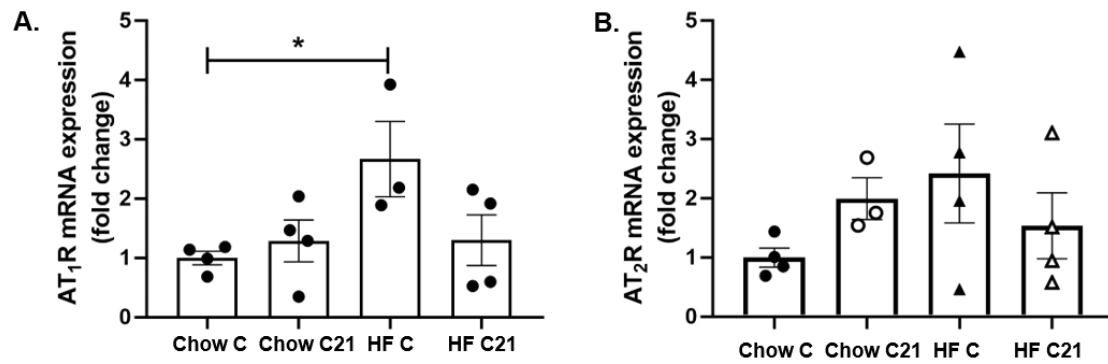
Supplemental Figure 1: Dot-blot graphs show mRNA expression of AT_1R (A) and AT_2R (B) in samples of abdominal aorta from Chow and HF mice treated or not with C21. Each result represents the mean ± S.E.M. (n=3–4). *$P<.05$ compared to the Chow C group (two-way ANOVA; Tukey's multiple comparison test).

Supplemental Figure 2
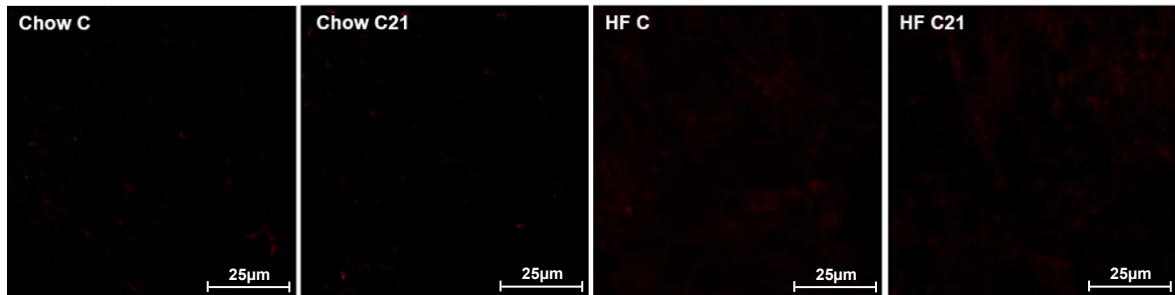
Supplemental Figure 2. Negative controls related with collagen I/III content in abdominal aortas.

Representative confocal images of negative controls for collagen I/III staining in segments of abdominal aorta. Projections were obtained from serial optical sections captured with a fluorescence confocal microscope (x63 objective, zoom 2).

Supplemental Table 1. Primers' sequences

Gene	Accession number	Forward primer (5´-3´)	Reverse primer (5´-3´)
Angiotensin II receptor, type 2 (*Agtr2*)	NM_007429.5	ATTGACCTGGCACTTC CTTTTG	CAATACAGGAAGGGATT AACACAGC
Angiotensin II receptor, type 1b (*Agtr1*)	NM_177322.3	TAACAGAGACCAGACA AGACACGC	ATGTCTCTTTGTTGGAG GGGGTG
TATA box binding protein (*Tbp*)	NM_013684.3	ACCCTTCACCAATGAC TCCTATG	TGACTGCAGCAAATCGC TTGG
Glyceraldehyde-3-phosphate dehydrogenase (*Gapdh*)	NM_001289726.1	TGACGTGCCGCCTGGA GAAA	AGTGTAGCCCAAGATGC CCTTCAG

Supplemental Table 2. Values of KCl and Phe-induced contractions in the abdominal aorta.

	Chow C	Chow C21	HF C	HF C21
KCl 60 mmol/L (g)	0.30 ± 0.02	0.34 ± 0.02	0.29 ± 0.02	0.33 ± 0.02
Phe 10^{-6} mol/L (g)	0.50 ± 0.05	0.51 ± 0.04	0.53 ± 0.04	0.51 ± 0.04

Data are expressed as mean $\pm$ SEM (n = 10).

Supplemental Table 3. E_{max}, pD_2 and AUC values of Ang II-induced contractions in the abdominal aorta.

	Chow C	Chow C21	HF C	HF C21
E_{max}				
Ang II	20.2 ± 3.8	17.7 ± 4.7	58.9 ± 6.0***	27.6 ± 4.3[###]
Ang II (PD123177)	77.1 ± 12.7[&&]	77.7 ± 15.6[&&]	55.4 ± 18.1	61.5 ± 16.4[&]
Ang II (HOE-140)	77.7 ± 18.6[&&]	92.7 ± 0.2[&&]	46.8 ± 16.9	88.0 ± 9.8[&&]
Ang II (A779)	71.2 ± 14.6[&]	67.6 ± 9.1[&]	43.5 ± 10.9	110.5 ± 4.1[&&&]
pD_2				
Ang II	7.5 ± 0.2	7.7 ± 0.2	7.6 ± 0.2	7.8 ± 0.1
Ang II (PD123177)	7.7 ± 0.2	7.9 ± 0.2	7.5 ± 0.2	7.4 ± 0.2
Ang II (HOE-140)	7.8 ± 0.2	8.0 ± 0.1	7.5 ± 0.2	7.7 ± 0.1
Ang II (A779)	7.4 ± 0.2	7.5 ± 0.2	7.2 ± 0.1	7.5 ± 0.2
AUC				
Ang II	61.0 ± 5.8	64.9 ± 20.0	178.5 ± 14.1***	100.2 ± 16.8[##]
Ang II (PD123177)	274.9 ± 48.9[&&]	285.6 ± 53.9[&&]	100.2 ± 16.8	234.3 ± 21.7[&]
Ang II (HOE-140)	287.7 ± 63.0[&&]	362.3 ± 4.3[&&&]	128.3 ± 73.8	313.0 ± 35.5[&&&]
Ang II (A779)	245.9 ± 68.0[&]	219.6 ± 36.2[&]	122.5 ± 27.8	365.3 ± 54.8[&&&]

E_{max} is the maximal contraction to Ang II expressed as % of contraction to KCl (60 mmol/L). pD_2 is the negative logarithm of the molar concentration of Ang II causing half maximal responses. AUC is the area under the curve to Ang II expressed as arbitrary units. Data are expressed as mean ± SEM (n = 10). ***$p< 0.001$ compared with Chow C mice. [##]$p<0.01$ and [###]$p<0.001$ compared with HF C mice (2-ANOVA; Tukey´s multiple comparisons test). [&]$p<0.05$, [&&]$p<0.01$ and [&&&]$p<0.001$ compared with their corresponding matched control group (1-ANOVA; Dunnett´s multiple comparisons test).

Supplemental Table 4. E_{max} values of Ang II-induced relaxation in the abdominal aorta.

	Chow C	Chow C21	HF C	HF C21
E_{max} Ang II	14.6 ± 1.0	19.3 ± 2.6	6.3 ± 1.9*	19.8 ± 2.4###
E_{max} (PD123177)	5.4 ± 2.6&&	8.9 ± 2.5&	7.5 ± 2.1	5.2 ± 2.9&
E_{max} (HOE-140)	1.2 ± 2.1&&&	7.1 ± 3.1&	3.6 ± 1.6	8.4 ± 1.7&&&
E_{max} (A779)	3.3 ± 1.2&&&	4.1 ± 5.9&	7.3 ± 6.5	3.0 ± 2.1&&

E_{max} is the maximal relaxation to Ang II in losartan pre-incubated aortic rings, expressed as % of relaxation to Phe (10^{-6} mol/L). Data are expressed as mean $\pm$ SEM (n = 10). *p<0.05 compared with Chow C mice. ###p<0.001 compared with HF C mice (2-ANOVA; Tukey´s multiple comparisons test). &p<0.05. &&p<0.01 and &&&p<0.001 compared with their corresponding matched control group (1-ANOVA; Dunnett´s multiple comparisons test).